

Co-funded by the



CEBAMA

➤ (Contract Number: 662147)

Deliverable D 1.06

Enhancements to state-of-the-art understanding for cement- clay interactions based on CEBAMA experimental studies (M42 – November 2018)

Editors: Francis Claret (BRGM), Erika Holt (VTT), Urs Mäder (UBern)

Date of issue of this report: 31.5.2019

Report number of pages: 34

Project co-funded by the European Commission under the Euratom Research and Training Programme on Nuclear Energy within the Horizon 2020 Framework Programme

Dissemination Level

PU	Public	X
PP	Restricted to other programme participants (including the Commission Services)	
RE	Restricted to a group specified by the partners of the CEBAMA project	
CO	Confidential, only for partners of the CEBAMA project	

Start date of project: 01/06/2015

Duration: 48 Months

TABLE OF CONTENTS

ABSTRACT.....	2
ACKNOWLEDGEMENTS.....	2
1 INTRODUCTION	3
2 ADVANCES IN UNDERSTANDING PHENOMENA IMPACTS.....	4
2.1 Thermal Impacts.....	4
2.2 Mechanical Impacts.....	8
2.3 Hydrological Impact.....	12
2.4 Chemical Impact.....	15
3 ADVANCES IN TESTING METHODOLOGY.....	24
3.1 X-Ray Diffraction.....	24
3.2 High-resolution PET scan	25
3.3 X-ray CT Imaging	27
4 UNDERSTANDING OF SCALE-EFFECT.....	29
5 CONCLUSIONS	31
6 REFERENCES	32

ABSTRACT

This report describes how the state-of-the-art understanding on cement-bentonite interaction has improved based on the experimental studies within the CEBAMA project. It complements the initial state-of-the-art literature review provided as Deliverable D1.03, published March 2016. The report covers both development of research methodologies and technologies, as well as information gained with respect to phenomenological processes affecting the interfaces of concrete-bentonite materials. Geochemical and physical evolution of the cementitious materials in a repository environment is described from various viewpoints.

ACKNOWLEDGEMENTS

This summary report of advances to the state-of-the-art has been compiled with contributions from the various institutes participating to workpackage 1 on experimental studies, including:

- KARLSRUHE INSTITUTE OF TECHNOLOGY (KIT), Germany
 - BUREAU DE RECHERCHES GEOLOGIQUES ET MINIERES ((BRGM), France
 - NATURAL ENVIRONMENT RESEARCH COUNCIL (NERC-BGS) UK
 - CENTRO DE INVESTIGACIONES ENERGETICAS, MEDIOAMBIENTALES Y TECNOLOGICAS (CIEMAT), Spain
 - STUDIECENTRUM VOOR KERNENERGIE- CENTRE D'ETUDE DE L'ENERGIE NUCLEAIRE (SCK CEN), Belgium
 - UJV REZ A.S. (UJV), Czech Republic
 - UNIVERSITY OF SURREY (SURREY), UK
 - CESKE VYSOKE UCENI TECHNICKE V PRAZE (CTU), Czech Republic
 - THE UNIVERSITY OF SHEFFIELD (USFD), UK
 - TEKNOLOGIAN TUTKIMUSKESKUS (VTT), Finland
 - HELMHOLTZ-ZENTRUM DRESDEN-ROSSENDORF (HZDR), Germany
 - UNIVERSITE DES SCIENCES ET TECHNOLOGIES DE LILLE –LILLE 1 (LML), France
 - UNIVERSIDAD AUTONOMA DE MADRID (UAM), Spain
 - AGENCIA ESTATAL CONSEJO SUPERIOR DE INVESTIGACIONES CIENTIFICAS (CSIC), Spain
 - AGENCE NATIONALE POUR LA GESTION DES DECHETS RADIOACTIFS (ANDRA), France
 - UNIVERSITAET BERN (UNIBERN), Switzerland
 - INSTITUT DE RADIOPROTECTION ET DE SÛRETÉ NUCLEAIRE (IRSN), France
-

1 INTRODUCTION

The CEBAMA project aimed at enhanced understanding of how the interactions of cementitious materials with buffer, backfill, host rock and closure materials within an underground repository impact upon long-term safety. The materials and their properties specified at the time of design and emplacement must ensure the safe evolution of the engineered barrier system when interacting with the surrounding environment. The specific objectives in CEBAMA were to understand how these chemical reactions affect water, solute and gas transport properties at the interface for various systems, including both low pH and ordinary Portland cement based cementitious materials combined with either crystalline rock, bentonite or OPA/COX/Boom Clay host rock.

The evaluation of the respective interactions was studied through using diverse methods:

- transport with tracers: dissolved gases, stable isotopes, trace components, radionuclide tracers
- use of tomography (PET) and tracers with ICP-AES, ICP-MS, IC, CRDS, gamma counting, IS
- characterization with SEM-EDXA, XRD, spectroscopy (EXAFS, XANES, XAS, FTIR, RAMAN), TGA, NMR.
- porosity measurement by 2D imaging and MIP, BET, μ -CT.
- swelling pressure, hydraulic conductivity, pozzolanic reactivity.

The methods used in the studies included laboratory experiments (e.g. batch experiments, diffusion cells, percolation including mechanical experiments) and in-situ assessment of interfaces with material sampling from Mont Terri, HADES, MHM, Tournemire, Josef, Japan URLs and dismantling large-scale experiments such as GRIMSEL in-situ FEBEX-DP and Lab HB6 cell.

A set of benchmark samples was also produced to provide inter-lab comparison on low pH concrete and cement paste. In the benchmark studies it was used various methods to assess mineralogical composition, diffusion coefficient, pore solution pH allowed comparison between methods and increased cohesion between individual experiments. Specific results of the benchmark test are reported separately (Deliverable D1.07).

The objective of this report is to provide insights about the overall advances to the state-of-the-art with respect to methods, as well as coupled process of thermal, hydro, mechanical, diffusion, physical properties and chemical evolution.

Table 1 represents the partners who were investigating different phenomena. Each class of phenomena is expanded in the next chapters to describe the advanced knowledge gained in the project. Specific details are reported individually by partners in the proceedings of the 4th Annual Workshop.

Table 1. Approaches used by project partners for various material studies. *T* = thermal, *H* = hydraulic, *M* = mechanical, *D* = diffusion, *P* = physical properties, *C* = chemical. *C_C_U*: CIEMAT, CSIC, UAM; “OPC” = OPC & NRVB.

Experiment	T	H&D	M	P	C
Low-pH/COx		UDL,BGS,HZDR	UDL,BGS	ANDRA	ANDRA
OPC/BoomC		SCK_BRGM		SCK_BRGM	SCK_BRGM
Low-pH/Toarc	IRSN	IRSN		IRSN	IRSN
OPC/Toarc	IRSN	IRSN		IRSN	IRSN
Low-pH/OPA		UNIBE		UNIBE	UNIBE
OPC/OPA		UNIBE		UNIBE	UNIBE
Low-pH/bent	UJV_CTU	UJV_CTU,C_C_U	UJV_CTU	C_C_U	UJV_CTU, C_C_U
OPC/bent	UJV_CTU	UJV_CTU,C_C_U	UJV_CTU	C_C_U	UJV_CTU, C_C_U
Low-pH/waters	UJV_CTU	KIT,C_C_U		KIT,VTT,USFD, USURREY, C_C_U	KIT,VTT,USFD, USURREY, C_C_U
“OPC”/waters	UJV_CTU	C_C_U		VTT,USFD, USURREY, C_C_U, TUDelft	VTT,USFD, USURREY, C_C_U, TUDelft

2 ADVANCES IN UNDERSTANDING PHENOMENA IMPACTS

2.1 Thermal Impacts

Experiments by IRSN included an OPC formulation using sulphate resistant Portland cement for Val d’Azergues. [Lalan et al., 2016; Dauzeres et al., 2017;] in contact with Toarcian Argillite. The important results in terms of exchange of soluble species, mineralogy changes causing microstructure modifications are summarized in the **Figure 1**. There was very low degradation of the CEM I material. The higher temperature seems to favour the carbonation, causing a small decrease of the total porosity contrary to the results in previous studies at 20 °C.

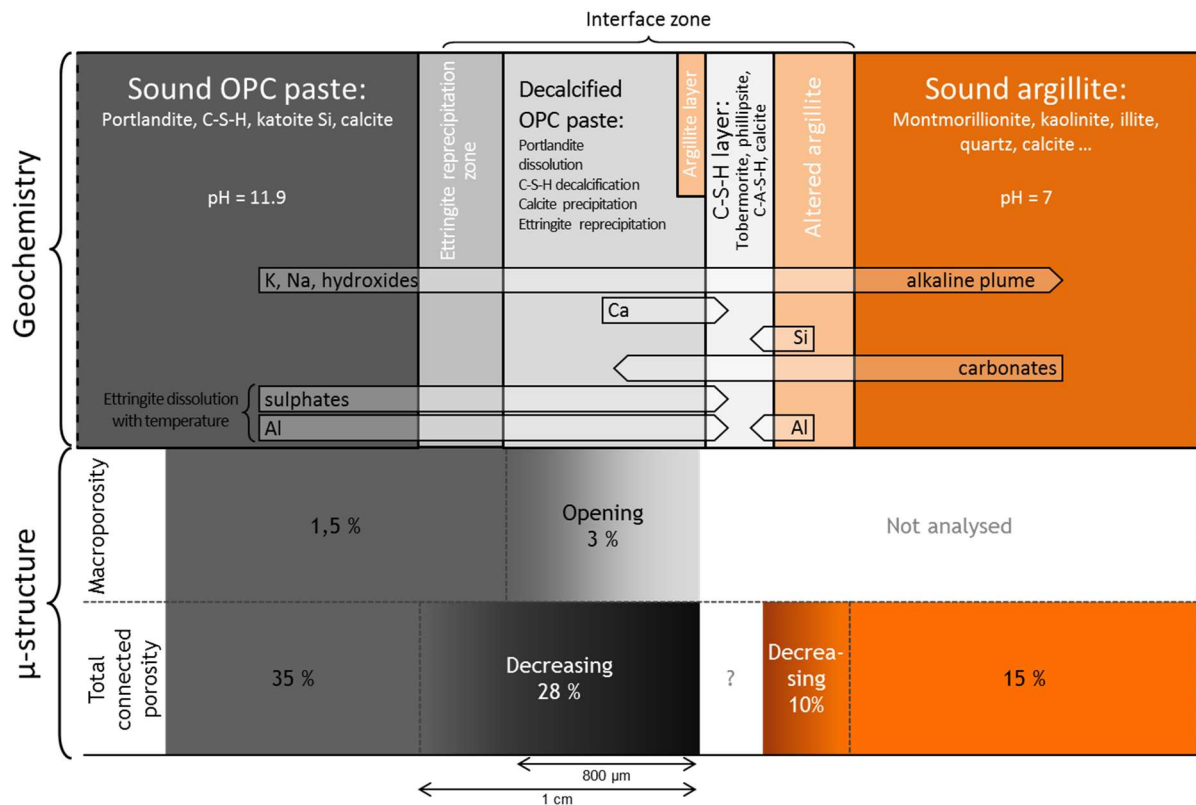


Figure 1. Summary diagram of the main mechanisms observed at the CEMI cement paste/clayey rock interface at 70 °C.

When similar results were done using low-pH binder named T1 [Codina et al., 2008] with 37% CEM I, 32.5% silica fume and 30% fly ash, there was a change in performance, as shown in **Figure 2**. This included:

- Decalcification of C-S-H close to the interface. This phenomenon is associated with the precipitation of M-S-H. This mechanism grew during the first year then stayed constant. No Brucite was observed.
- Porosity opening in cement matrix due to decalcification process. After a year of interaction, the porosity in the decalcified zone increased from 15 to 50%.
- In comparison to OPC, clay-phase dissolution was not clearly observable with the CEMI, certainly linked to the chemical transition during the cement paste hydration.
- The cement alteration is more important for the low-pH material (decalcification, M-S-H precipitation causing porosity opening) compared to the CEM I formulation.

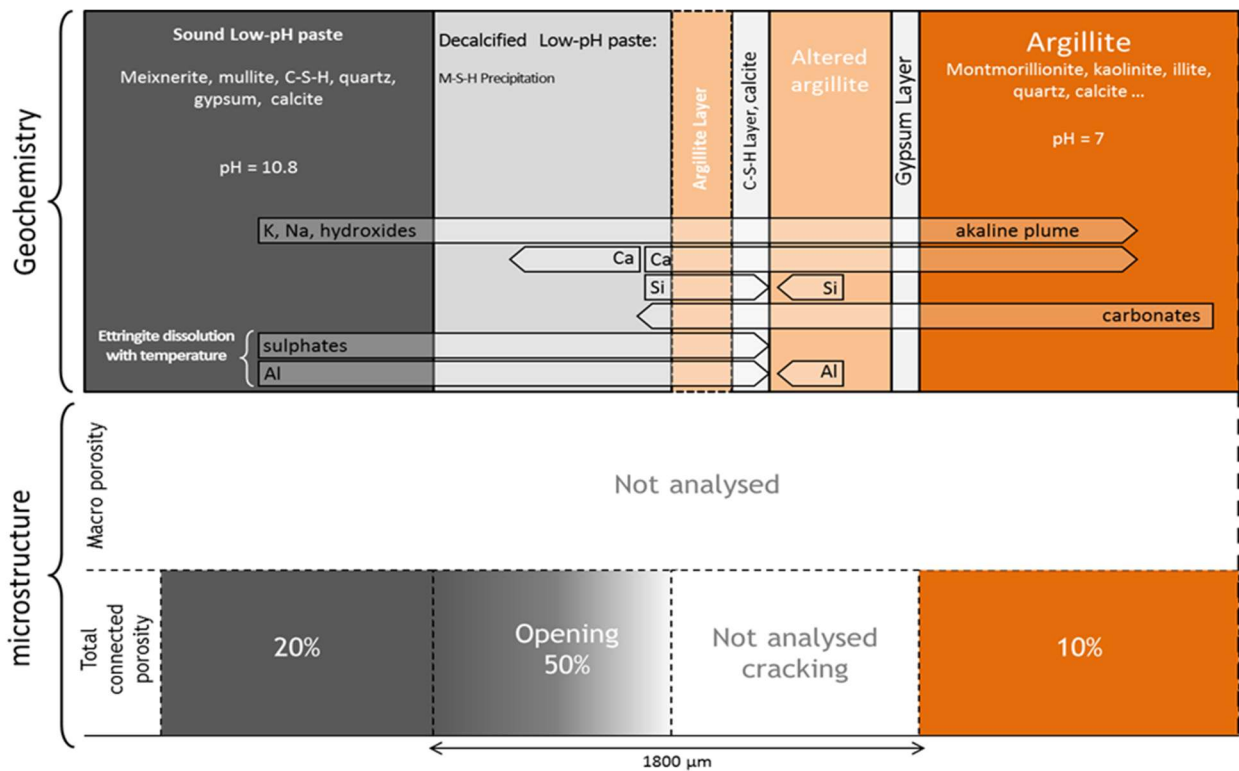


Figure 2. Summary diagram of the main mechanisms observed at the Low-pH cement paste/clayey rock interface at 70 °C.

In the case of OPC (**Figure 1**), classically, the modelling planned (whatever the temperature) the precipitation of zeolites at the interface, especially in the clayey rock. But this numerical result was never verified experimentally in the interface experiments, controlled by diffusive exchanges. For the first time, the precipitation of K-phillipsite was clearly characterized chemically and structurally in the three experiments carried out with CEM I cement in the tournemire URL. The densification of this zeolite layer was also well demonstrated at 1, 2 and 5 years of interaction, mainly due to the high temperature conditions.

In the case of low-pH (**Figure 2**), characterizations exhibit a degradation higher than the CEM I with a strong decalcification associated to a Mg-enrichment due to the precipitation of M-S-H phase. The precipitation of M-S-H is explained (in addition to the high temperature) by the alkaline transitory, when the cement is freshly poured in contact with the rock, before to acquire, after several weeks, the chemical properties of a low-pH. The global chemical evolution causes a porosity opening in opposite to the relative decline in the CEM I material.

This study at 70 °C confirms the higher reactivity of low-pH cementitious materials in contact with a clayey environment, as observed at 50 °C or 20 °C in the literature

Another series of experiments by the team of UJV-CTU in the Czech Republic looked at the evolution of uniaxial strength and rigidity (elasticity) at various temperatures. Their results showed an impact on both properties based on both temperature and cement chemistry (**Figure 3**).

Compressive strength measurements on the OPC – the initial uniaxial compressive strength value (non-aged samples) of the OPC was determined, following recalculation, to be around 60 MPa [Večerník, 2016]. The results revealed that temperature exerts a significant effect on both compressive strength and elasticity. Almost all the results related to the same temperature (10 °C or

95 °C) follow the same trends. Compressive strength decreased in the case of “heated” (95 °C) OPC to 60% (approx. 36 MPa) of the initial value while at a temperature of under 10 °C compressive strength was seen to slightly increase over time (to around 120%, i.e. to approx. 72 MPa). In addition, elasticity decreased with respect to all the heated samples. While the influence of the presence of bentonite appears to be less important than that of temperature, the results indicate the protective role of bentonite under 95 °C (elasticity is less affected). It must, however, be emphasised that the conclusion regarding “elasticity” is indicative only [Vašíček, 2018].

Compressive strength measurements on the RPM - hardening is observed for all types of samples/ ageing procedures after 9 months. Value from “humid air at 10°C” (black empty triangle) can be taken as a result of “hardening under normal condition”, with increase to 140% (approx. 112MPa after recalculation). In such cases it could be concluded that all other ageing conditions provided harder samples with an increase up to about 180% (approx. 144MPa) for “hot water” (95 °C + GW Josef). Figure shows that temperature (10 or 95 °C) have also certain influence on strength evolution, in that the “hot” environment produced harder samples after 9 months. As all results from “environment without bentonite” (initial and all empty triangles) created linear progression, it can be estimated that elasticity remained unchanged for such samples/ageing environments (i.e. without bentonite). Contrary to this, samples from “bentonite suspension” have lost part of their elasticity [Vašíček, 2018].

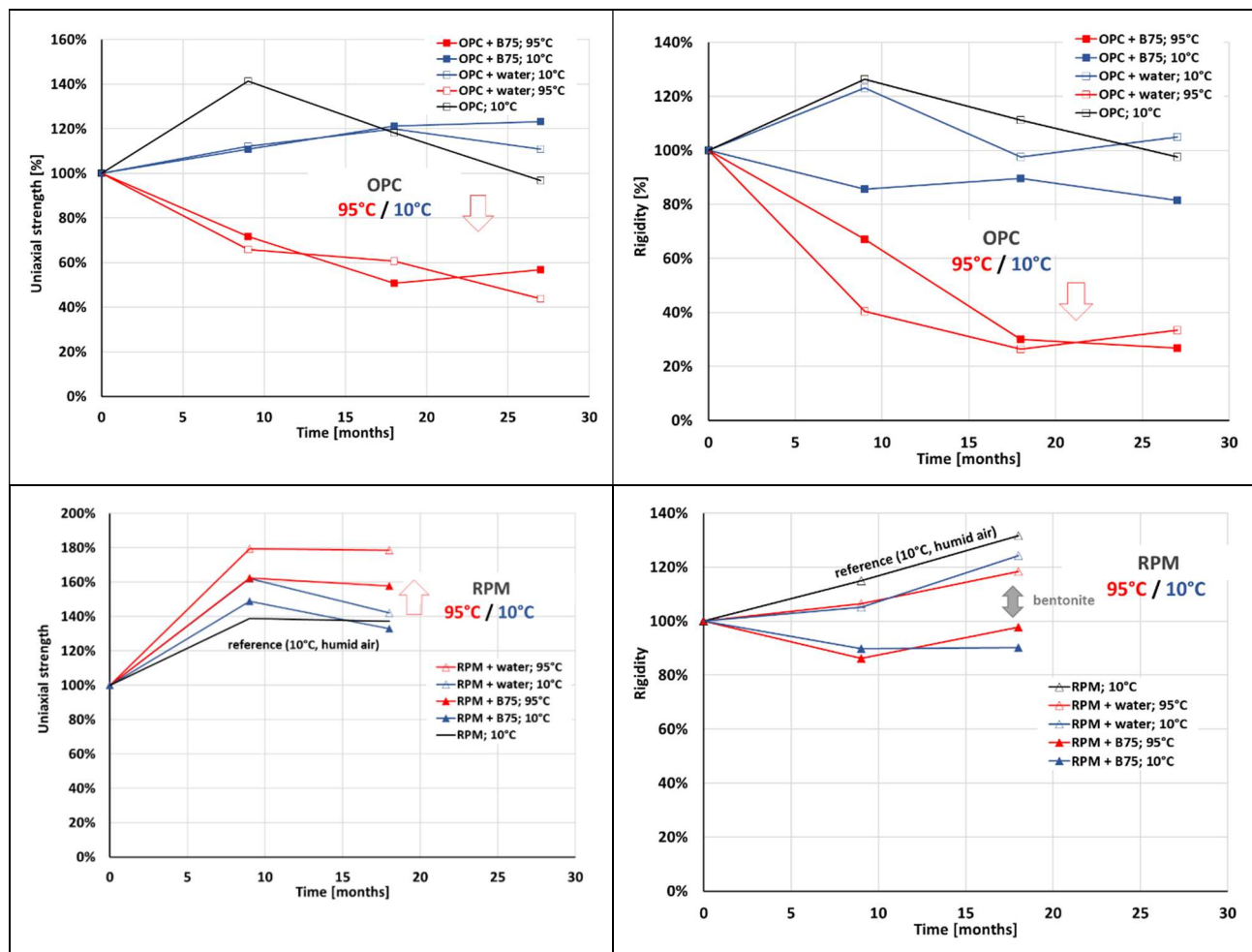


Figure 3. Time evolution of uniaxial strength (left) and rigidity (right) of OPC and RPM samples. (UJV-CTU)

2.2 Mechanical Impacts

Another example of the mechanical impacts of the material interfaces was demonstrated by BGS (UK) and Andra (France). Their joint experiment evaluated the interface made of clay-rich Callovo-Oxfordian claystone (COx; UA) or high carbonated variety of COx (USC) in contact with a TL variant of a ternary blend concrete. The disposal concept is shown in **Figure 4**, with example results in **Figure 5**. The uniaxial strength of the concrete samples increased during curing, as expected. However, the rate of strength increase was slower than previously published. Considerable strength difference was seen between the UA and USC varieties of COx (a, c). The USC has a shear strength in excess of 20 MPa, whereas the UA variety had a strength closer to 6 MPa. The high clay content variety (UA) showed natural variation in yield, peak, and residual shear stresses (b, c). The two samples of concrete tested showed considerably different shear strengths. In one, a modest strength of approximately 2 MPa was seen, whereas in the other it was approaching 15 MPa.

Generally, interfaces showed very low strength similar to the residual strength of intact COx. However, despite the observation that the interface had little strength, there was evidence that the strength of the interface increased with time for the UA variety of COx (a, c, d) with a modest strength increase over a year. It should be noted that the test conducted at approximately 40 weeks showed abnormally high strength that may have derived from accidental drying of the sample. The story in the USC COx (b) is not as clear with the initial test of the fresh material showing the interface had strength, the test after six months showed no strength, and the test after one year showed enhanced strength.

From the results (**Figure 5a**), the general summary can be made that there was a reduction of flow as shear stress increased resulted in a near linear relationship. This suggests that a shear movement along the interface acted as an effective self-sealing mechanism. **Figure 5b** also indicates the formation of a shear zone parallel with the interface has resulted in enhanced flow. As the concrete aged interface flow reduced for the UA/TL interface but increased in the USC/TL case. Differences were also seen whether the initial interface was smooth or rough. Therefore it can be seen that shear stress, interface roughness, and chemical aging of the concrete are a clear control on interface transmissivity. The resultant fracture topology showed that the characteristics of the fracture surface changed as the interface matures. This is reflected in changes in strength and flow. Despite changes in strength and flow behaviour, no discernible change in geochemistry was seen during petrographic analysis to explain these changes.

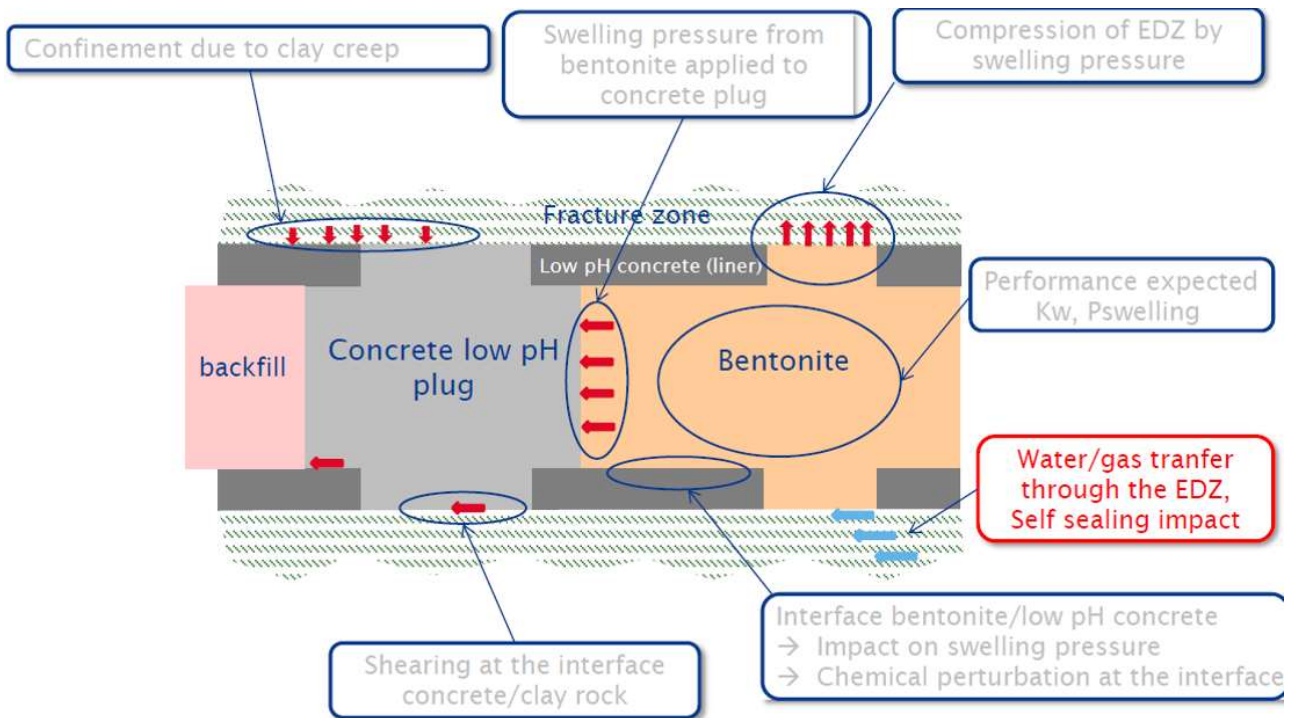


Figure 4. Conceptual model showing the disposal concept of Andra in a horizontal tunnel at depth in Callovo-Oxfordian claystone (COx). Highlighted by red arrows of the mechanical stresses generated by convergence of the tunnel and swelling of the bentonite seal. This results in stresses between the COx and concrete plug, as well as stresses between the low pH concrete liner and concrete plug. The blue arrows highlight the flow of fluids along the system.

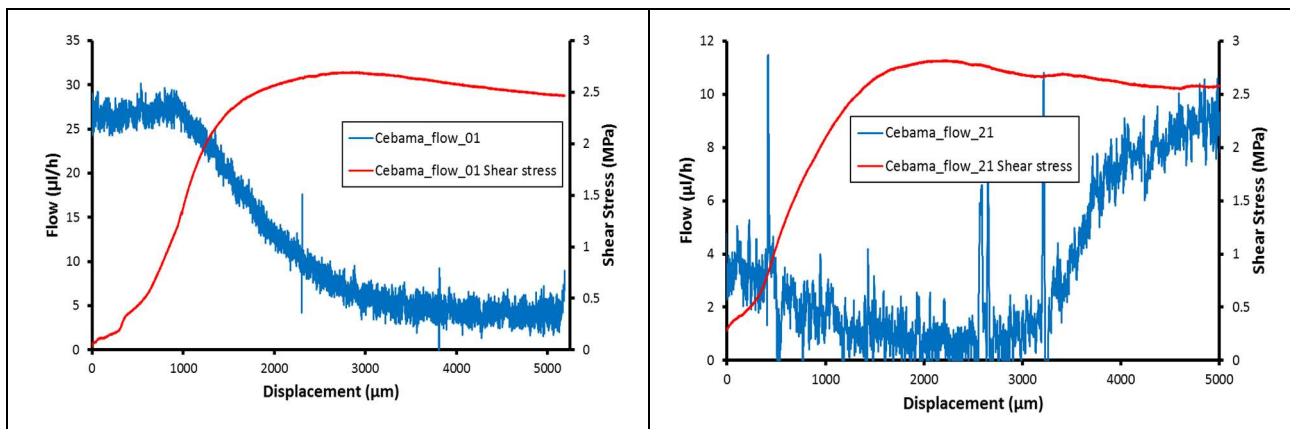


Figure 5. Indicative results from flow experiments in actively shearing concrete/Callovo-Oxfordian claystone interfaces. One order of magnitude reduction in flow is seen as a result of shear movement of the interface in many experiments (left) as the shear stress increases along the interface. In some tests prolonged shear resulted in increased flow (right) as a shear zone formed parallel with the interface.

UDL in collaboration with Andra evaluated the hydromechanical properties of interface. A series of triaxial direct shear tests under different values of confining pressure from 2 MPa to 12 MPa and different values of pore pressure from 1 MPa to 4 MPa have been carried out. The specific values of confining stress and pore pressure are chosen such that their difference is the same between a pair of tests respectively with and without injection water pressure. The objective is to investigate the effect

of pore pressure on the shear strength of interface and to check the validity of effective stress concept for interfaces.

The representative stress-strain curves obtained in the test with a confining pressure of 12 MPa, an injection water pressure of 4 MPa are shown in **Figure 6**. Positive stress denotes compression and negative strain means dilation. In **Figure 6(a)**, there is a nonlinear relation between the shear strain and shear stress even during the first stage of loading. However, the radial strain or the diameter change (ΔD) remains very small during the first stage of shearing. It means that the shear strain does not induce interface opening or closure when it is less than some critical threshold. After that threshold, we obtain an important negative radial strain. The shear strain induces a significant closure of interface, probably due to the degradation of asperities in the interface zone.

The image of the tested sample is presented in **Figure 6(b)**. One can see that the two semi-cylinders are clearly slipped each to other but the two parts are still hold together due to the compressive normal strain (compaction) of the interface. The two surfaces of the tested sample are shown in **Figure 6(c)**. Frictional traces of shearing at the surface can clearly be observed. In addition, the claystone powders are found on the sheared surfaces of both semi-cylinders, due to the fact that the claystone is much weaker and more sheared than the concrete in the two-material system. Some claystone powders can be pushed into concrete pores, leading to a decrease of the permeability of the interface zone.

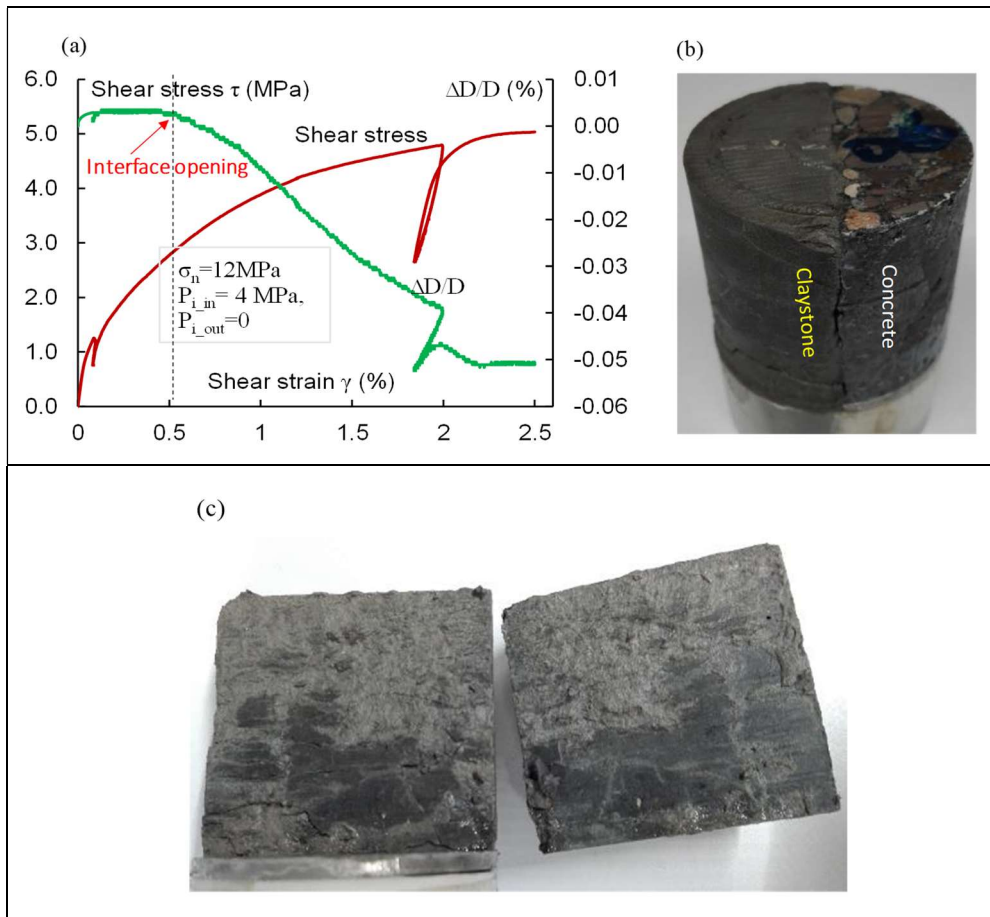


Figure 6. Shear stress/strain diagram (a) of claystone-concrete sample (b), and post testing split (c).

Upscaling further, Andra also used in-situ experiments to understand the long term chemical interactions between low-pH materials with their potential natural environment of a clay host rock, including ventilation from the gallery.

The situ test (**Figure 7**) has been realised in the French Underground Research Laboratory (URL) in Bure (Meuse/Haute-Marne, France), at 500 m depth in the Callovo-Oxfordian claystone layer. It has been designed to be representative of the operating conditions of a geological disposal facility and to assess the evolution of the concrete with two type of boundary conditions: (i) the face in contact with ventilation air which evolve under atmospheric conditions and is submitted to drying and atmospheric carbonation; (ii) the concrete/clay interface where hydro-mechanical properties evolve mainly due to geochemical interaction between both materials. The studied cementitious materials are “Low Hydration Heat/Low pH concretes”, specifically designed for plugs and seals. Two formulations were studied. Both recipes fulfil the requirements regarding the physical and the chemical expectations. Both are based on a ternary blend with Clinker, Silica Fume and Fly Ash or Blast Furnace Slag. To follow the evolution of their physical properties with time, the concrete elements are monitored.

Figure 8 shows examples of the evolution of temperature with time after casting. Measured temperature are in accordance with lab scale experiments on these two blended cements. There is a small impact on the temperature evolution at the surface considering the boundary conditions (the maximum temperature reached is not more than 10–12 °C higher than the ambient temperature at the surface of the walls, compared to the ~17 °C in the bulk). The modelled temperature transient in relation to the hydration of the TCV blended cements is correctly reproduced. Due to the very low kinetic of hydration of the slag, some discrepancies are still noticed (temperature maximum reached not as high as measured), leading to differences between measurements and simulations close to 20%. Adiabatic measurements on the slag alone could confirm the accuracy of the fitting.

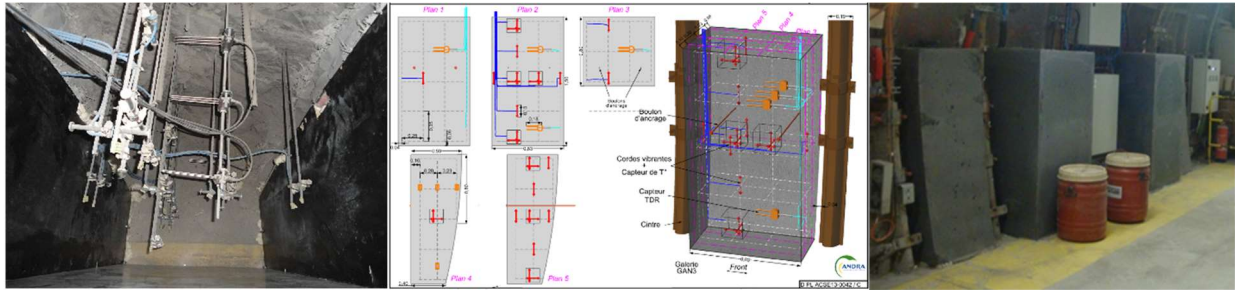


Figure 7. Views of the in situ test. (Andra)

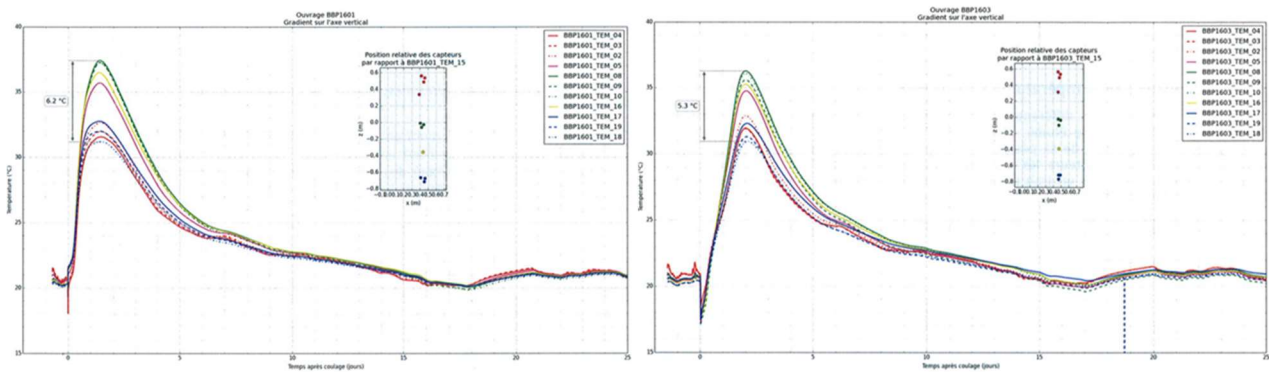


Figure 8. Temperature evolution of the thick walls T_{cv} (left) and T_L (right). (Andra)

2.3 Hydrological Impact

Several partners studied the impact of material interfaces on hydraulic properties, especially pertaining to diffusion and permeability.

KIT (Germany) performed through-diffusion experiments of HTO and $^{36}\text{Cl}^-$ in young low-pH cementitious materials to derive diffusivity values for low-pH cement pastes not available in the literature. As illustrative example, the accumulated amounts (mol) of HTO and in the low reservoir and their diffusive fluxes during the diffusion through two RPM samples are shown in **Figure 9**. Transport parameters of HTO and $^{36}\text{Cl}^-$, such as, the effective diffusion coefficient D_e [m^2/s], the capillary porosity, ε [-], and the rock capacity factor, α [-], were obtained by inverse modelling considering Fickian diffusion and using the finite element code Comsol Multiphysics 5.3 to solve the partial differential equations. To verify the applicability of the relationship between porosity and effective diffusivity, the fitting of the experimental data was carried out using two approximations: a modified Archie's law and a multiporosity approach developed in the National Institute of Standards and Technology “NIST” [Bentz et al., 2000].

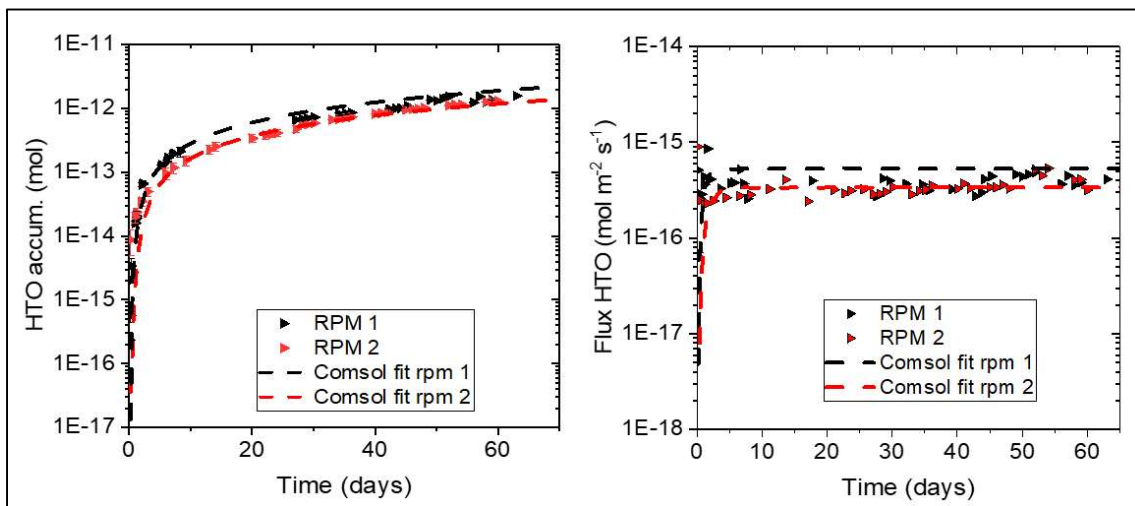


Figure 9. Accumulated amount of HTO in the low reservoir vs. time and its diffusive flux during diffusion experiments through cebama paste “RPM”. $[\text{HTO}]_0 = 1.86 \cdot 10^{-9} \text{ M}$. Background electrolyte was equilibrated water. (KIT)

The team of CIEMAT, UAM and CSIC (Spain) conducted gas permeability and hydraulic conductivity measurements in aged samples taken from the shotcrete plug within the FEBEX in-situ test. Their results (**Figure 10**) showed that the increase in confining pressure did not modify gas permeability, which would be an indication of the absence of microcracking. The gas permeability was higher as the samples had less water content and lower degrees of saturation. The hydraulic conductivity values obtained were in the order of 10^{-10} m/s , higher than the initial values of the shotcrete plug S1 at 28 days curing ($4.3 \cdot 10^{-11} \text{ m/s}$).

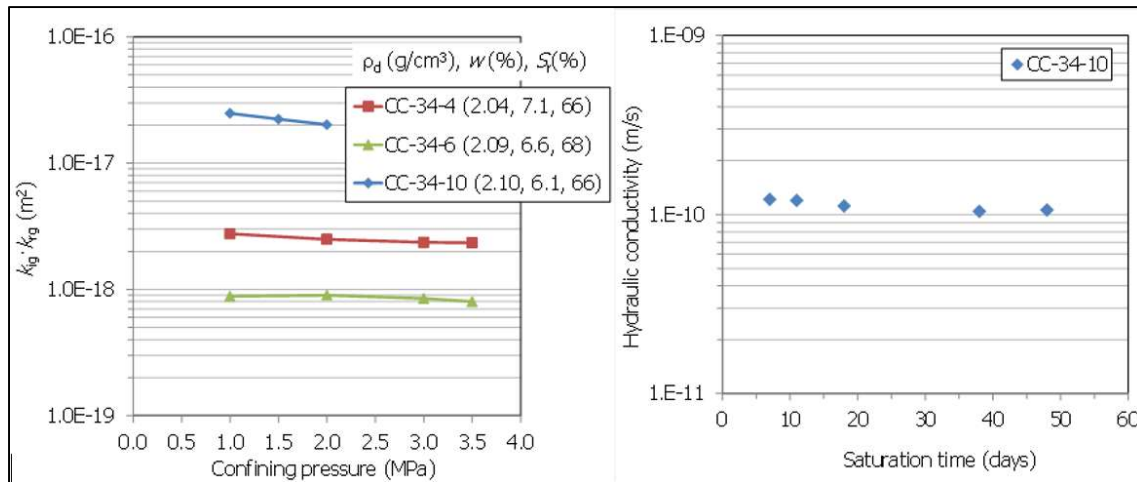


Figure 10. Effective gas permeability with increasing confining pressure. The values are the average of all steps under the same confining pressure (left). Hydraulic conductivity of sample CC-34-10 over time (right). (CIEMAT-UAM-CSIC)

The UJV_CTU team performed through-diffusion (TD) experiments of HTO (^3H , ~ 5 nM) and chloride (~ 15 – 20 mM, marked by ^{36}Cl of 55 – 60 μM) on samples that were under temperature and ageing load, see **Figure 11**. The HTO effective diffusion coefficients of the OPC samples increased with temperature load (preceding the diffusion experiment itself) by approximately in one order of magnitude (from 3 – $7 \cdot 10^{-12}$ to 2 – $5 \cdot 10^{-11}$ m^2/s) which may have been related to the dissolution of the material under higher temperatures as well as a decrease in elasticity (microcracks) which lead to changes of a geometry of a diffusion pathway; on RPM samples, there is no significant difference – all effective diffusivities are in the same order of magnitude ($D_e = 2$ – $6 \cdot 10^{-13}$ m^2/s). The sample ageing procedure (approx. 9, 18 or 27 months) in pressure vessels did not confirm any dependency on diffusion parameters. The chloride-36 migration was strongly retarded in OPC samples and the evaluation of diffusion coefficients fitting a K_d , porosity “ ϵ ” or geometrical factor “ G ” became challenging. On contrary, the chloride anions were strongly repulsed from RPM samples (no decrease of chloride-36 concentration activity in the inlet reservoir) and no breakthrough (in the outlet reservoir) was observed even after 200 days in all series (except of samples that came from series “RPM+GW Josef at 95°C ”, where $D_e < 5 \cdot 10^{-13}$ m^2/s). Therefore, we concluded the diffusion process of chloride on RPM samples is very slow (in all remaining series that were under different interactions for approx. 9 months: $D_e < 10^{-13}$ m^2/s) and there are no retardation processes of chloride on RPM samples expected ($K_d = 0$).

Obtained data are not fully comparable to literature survey [Vehmas, 2016] due to different materials used and different experimental conditions, the literature data shows D_e values in order of magnitude 10^{-12} m^2/s .

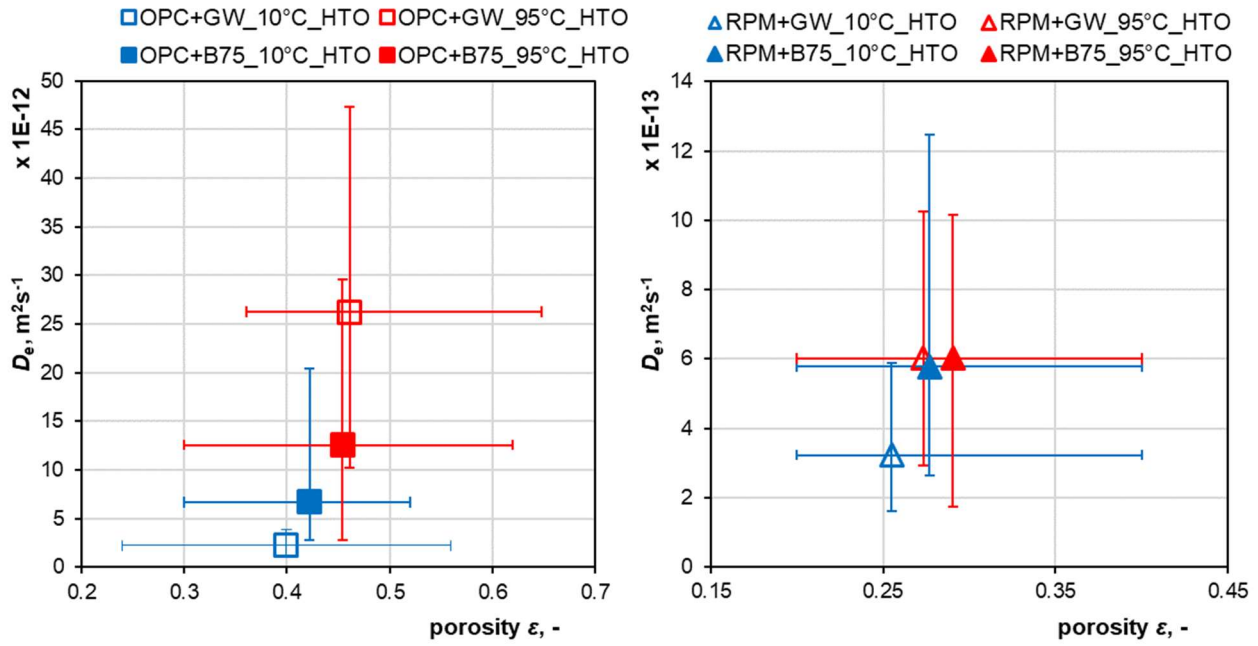


Figure 11. Effective diffusion coefficient of HTO on OPC and RPM samples: dependency on the porosity of the samples; each series with OPC (RPM): mean value from 7(4) TD experiments. (UJV-CTU)

Another set of hydraulic conductivity assessments were done by SCK-CEN and BRGM, on aged backfill concrete in contact with Boom Clay compound samples (**Figure 12**). [Phung et al.; in preparation]. The composite permeability slightly decreased. However, the change compared to the reference permeability of clay can be negligible taken into account the uncertainty of permeability measurement in the percolation experiment. Both precipitation and dissolution might simultaneously occur at the interface. Some precipitation of calcium carbonate could occur in the clay side due to carbonation resulting in a porosity drop. On the other hand, dissolution of some phases in clay due to advective (and also diffusive) flow could increase the porosity of clay which compensate the porosity decrease due to carbonation. Therefore, a significant change in permeability was not observed, though in other cases when using contact to Opalinus Clay, a reduction was observed. For the backfill side, similar phenomenon could happen. However, these change in microstructure could be too small to interfere with the permeability.

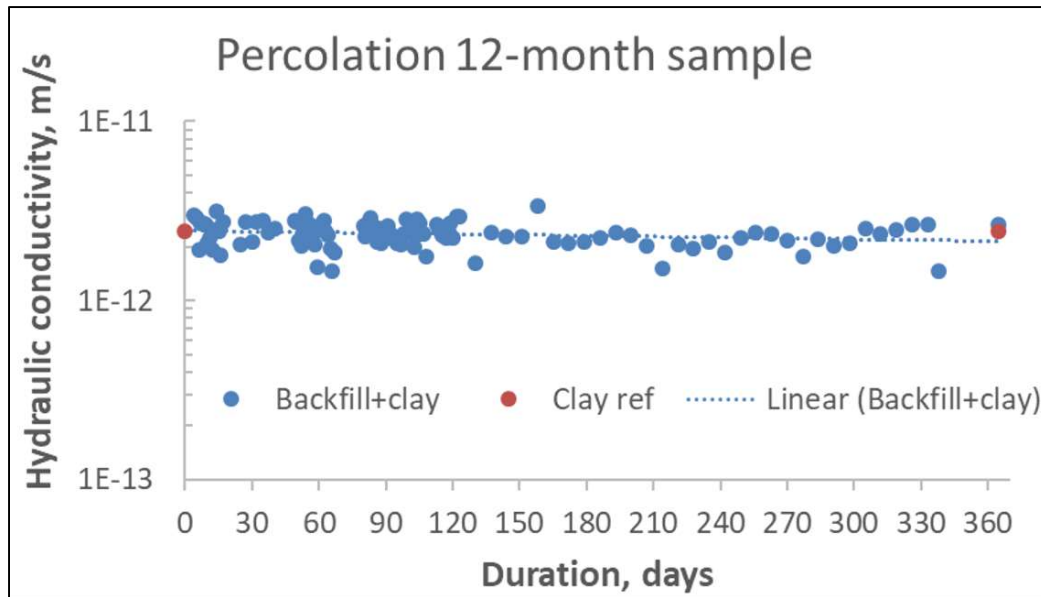


Figure 12. Permeability evolution during percolation experiment for backfill – Boom Clay interface. (SCK-CEN, BRGM)

2.4 Chemical Impact

To understand the chemical evolution of the concrete in contact with groundwater containing leachate from bentonite for long-term evolution safety, VTT (Finland) and USFD (UK) studied the leachate of cementitious materials both young and aged in different groundwater compositions representing granitic, clay and saline environments. Detailed analysis was done of mineralogical changes and mass transfer, showing how OH-release has an impact to the clay barrier. Examples of these results are shown in **Figure 13** and **Figure 14**.

According to Figure 13, groundwater composition has a large effect on leached hydroxyl ions compared to ion-exchanged water. The amount of leached hydroxyls were similar in pristine saline groundwater and bentonite affected groundwater. Calcium/silica -ratio of the binder had also clear effect on released hydroxyls. The amount of released hydroxyl was insignificant at calcium/silica -ratios below 0.8 in ion-exchanged water. In saline groundwater, hydroxyl release became insignificant at the calcium/silica -ratios 1.2-1.0. Experimentally measured values were comparable to thermodynamically modelled values [Vehmas et al. 2016, Vehmas et al. 2017, Vehmas et al. 2019]. Measured values enable quantitative estimations on cementitious materials effect on barrier properties, as presented in [Koskinen, 2014] or [Vehmas et al, 2017].

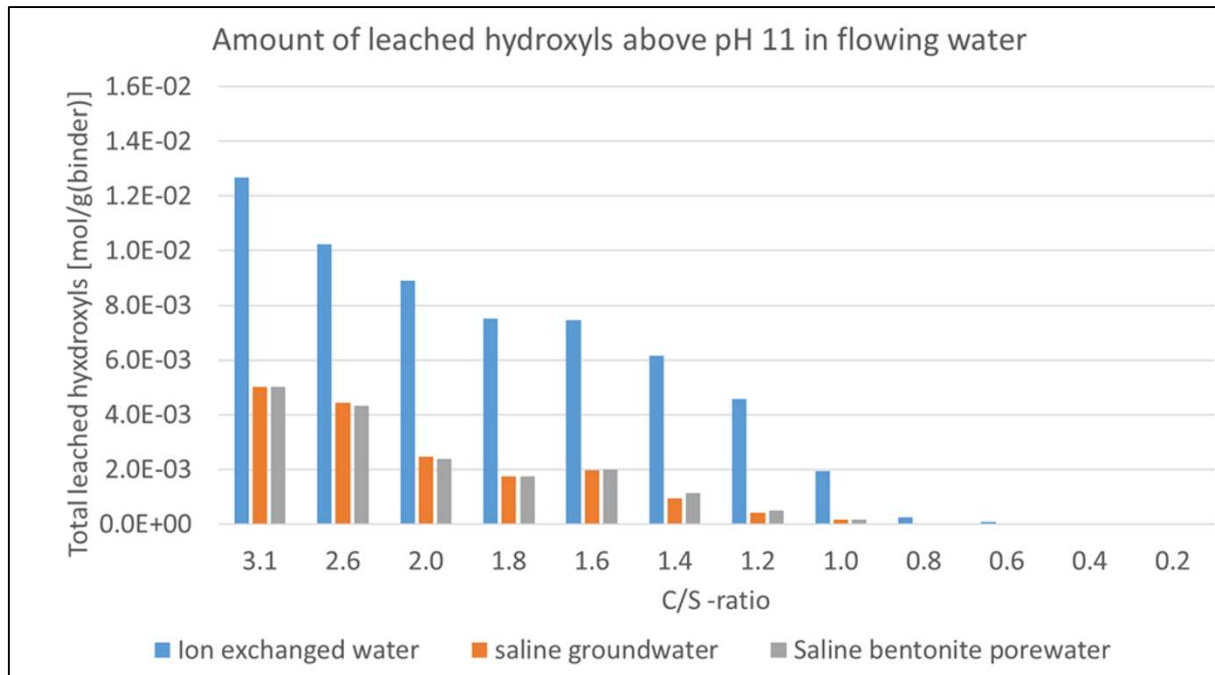


Figure 13. Experimentally determined amount of leached hydroxyls above pH 11. Below pH 11, bentonite is considered as stable. (VTT)

In Figure 14, the mineralogy of NRVB (Nirex Reference Vault Backfill, high pH) cement was influenced strongly by both saline and clay groundwater compositions, but was not affected significantly by the granite groundwater. The presence of sulphur in the groundwater solutions (4 and 15 mmol L⁻¹ for saline and clay, respectively) was the main source of the mineralogical changes; sulphur was removed from saline and clay solutions by the cement, which promoted the formation of ettringite ($\text{Ca}_6\text{Al}_2(\text{SO}_4)_3(\text{OH})_{12} \cdot 26\text{H}_2\text{O}$).

An increase in DTA peaks and XRD reflections associated with the presence of ettringite was observed for saline and clay solutions (Figs 14a and b, respectively) and there was an increase in the ²⁷Al NMR signal representative of ettringite for these solutions (Fig. 14c). The insert in Fig. 14c shows an SEM image confirming the presence of ettringite needles. There was a reduction in the Ca/Si ratio of the C-S-H within NRVB in saline and clay groundwaters, as determined by ²⁹Si NMR analysis (Fig. 14d), which suggests that C-S-H was decalcified. Since this was not observed in the granite groundwater where no additional ettringite was formed, this suggests that ettringite formation was facilitated by the interaction of sulphur in groundwater with Ca (and Al) in C-S-H.

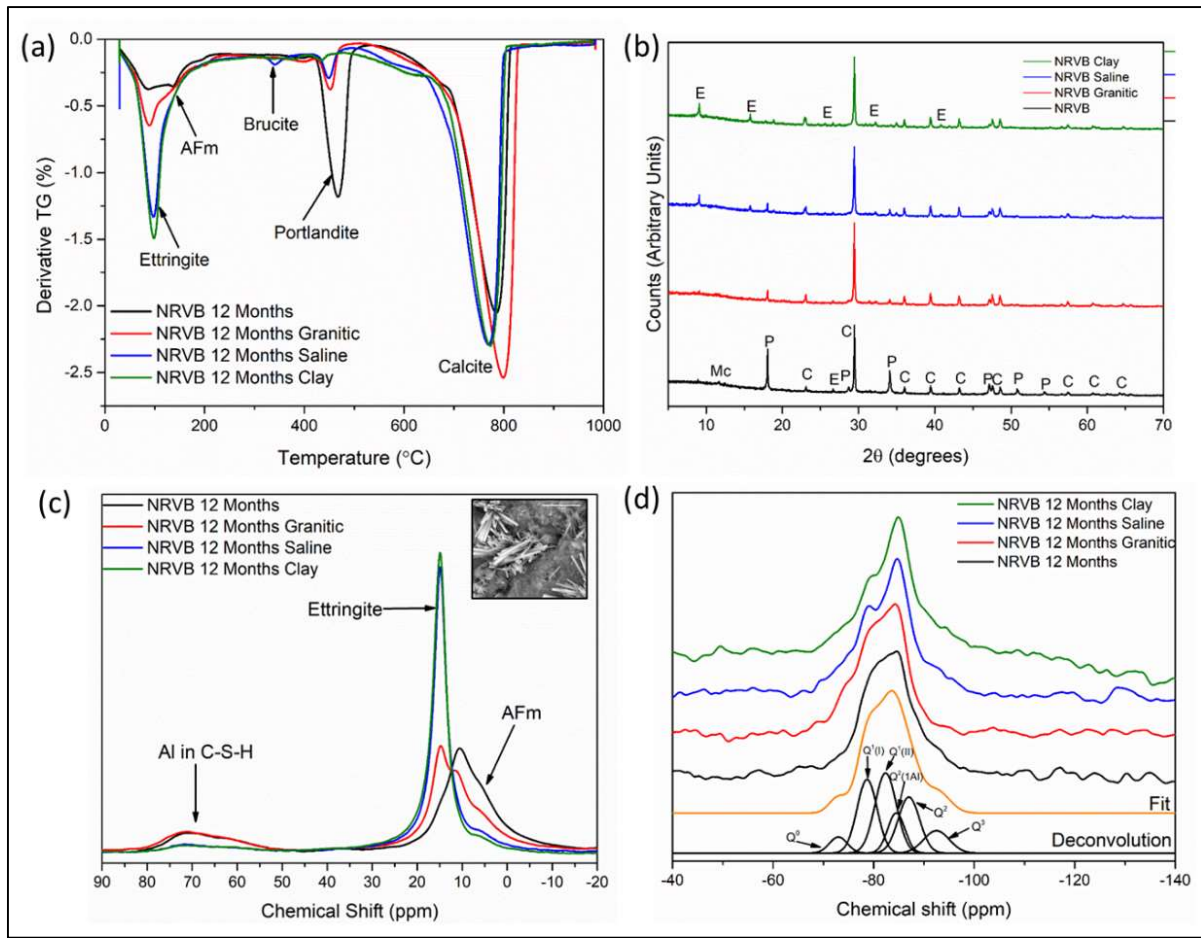


Figure 14. Comparison of NRVB samples exposed to three different groundwater solutions for 12 months, and comparison to blank (i.e. non-groundwater contacted) material: (a) analysis by TGA; and (b) analysis by XRD. E = ettringite, M = monocarboaluminate, P = portlandite, C = calcite; (c) ^{27}Al NMR analysis; insert in (c) shows SEM images of ettringite needles; and (d) ^{29}Si NMR analysis and deconvolution. (USFD)

In addition to mineralogical changes at the cement-groundwater interface, the impact of cementitious materials on the surrounding groundwater chemistry was also studied (University Surrey). The diffusion studies, **Figure 15**, allowed the alteration of groundwater pH to be observed, following submersion of cement blocks of varying blends (CEMI, GGBS:OPC, NRVB and CEBAMA reference blend). From **Figure 16**, it is seen that the groundwater pH increased to greater than pH 11 following one day's interaction with cement. The higher pH, greater than pH 12, was achieved by CEMI and NRVB cement blends.

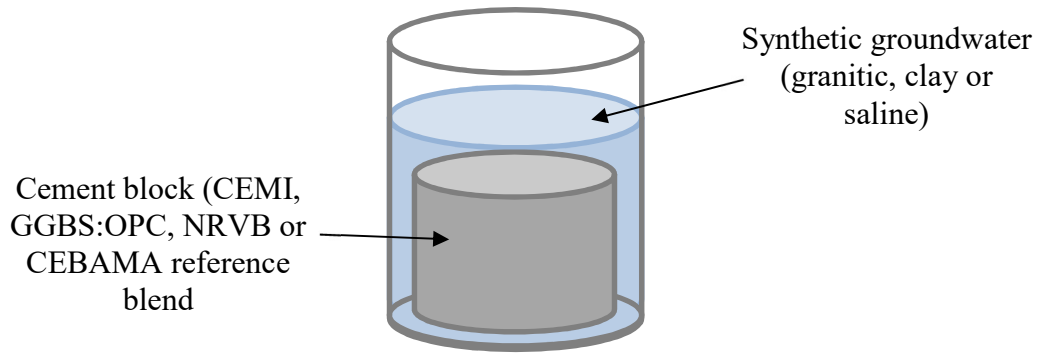


Figure 15. Set-up for cement-groundwater diffusion experiments. (Surrey)

Changes to groundwater chemistry, particularly anion content was monitored over a period of five months (**Figure 17**). The results are expressed as percentages by comparing the cement-groundwater sample composition with the baseline groundwater (no interaction with cement), as shown in Equation 1.

Equation 1.

$$\text{Solution chloride (\%)} = \left(\frac{[\text{anion}] \text{ within cement} - \text{groundwater sample}}{[\text{anion}] \text{ within baseline groundwater sample}} \right) \times 100$$

The four cement blends studied can be divided into two groups, high-pH (CEMI and NRVB) and low-pH (GGBS:OPC and CEBAMA), dependent on the behaviour of uptake or leaching of anions. Irrespective of the groundwater, the greatest uptake of solution chloride and sulphate was observed for CEMI and NRVB. An increase in solution sulphate was observed when GGBS:OPC and CEBAMA interacted with granitic groundwater. The higher sulphate content of these cement blends is believed to be the reason for this.

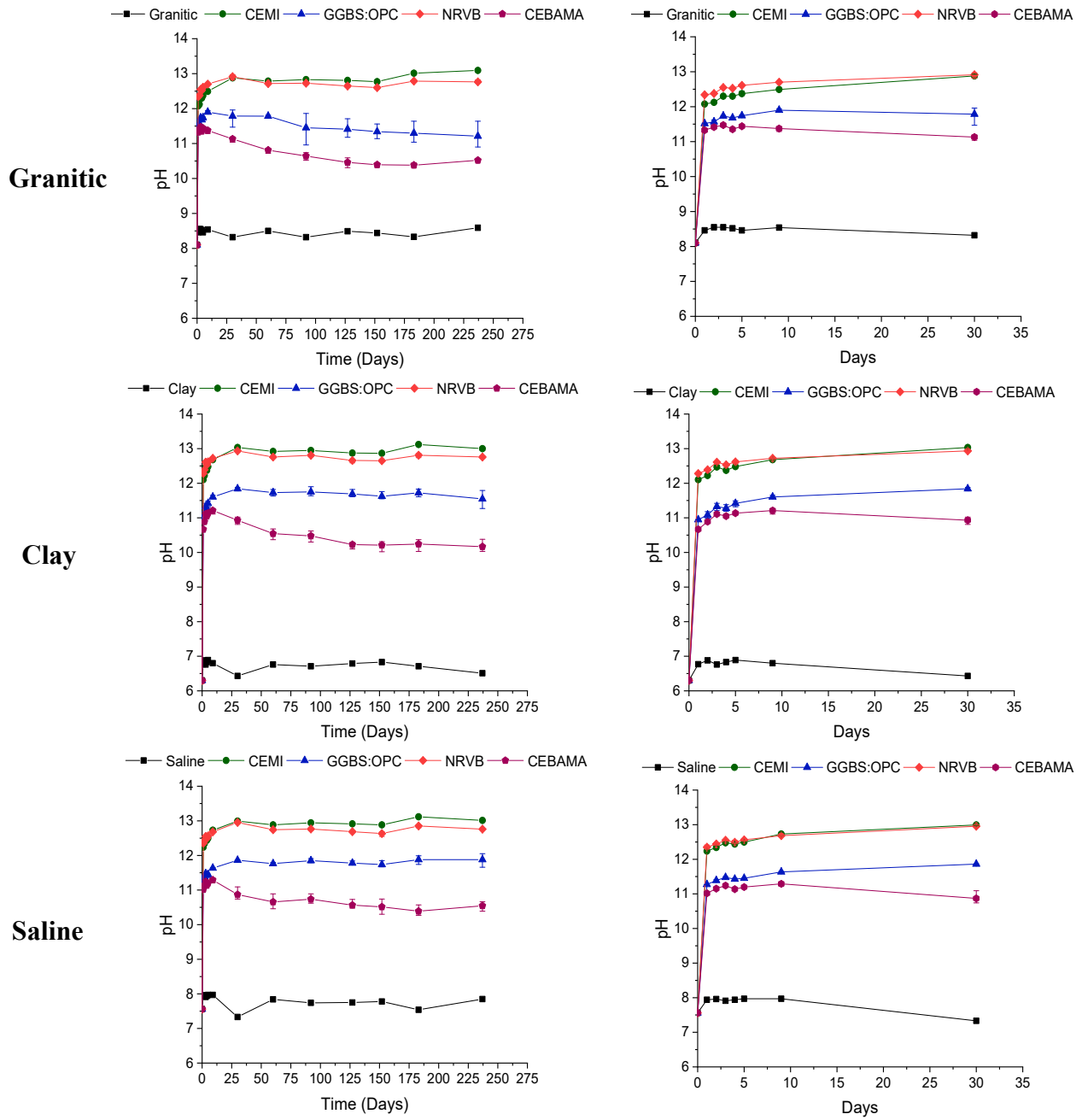


Figure 16. Changes to granitic, clay and saline groundwater pH following interaction with cementitious materials. Left: 237 days interaction, right: expanded 0–30 day's interaction.

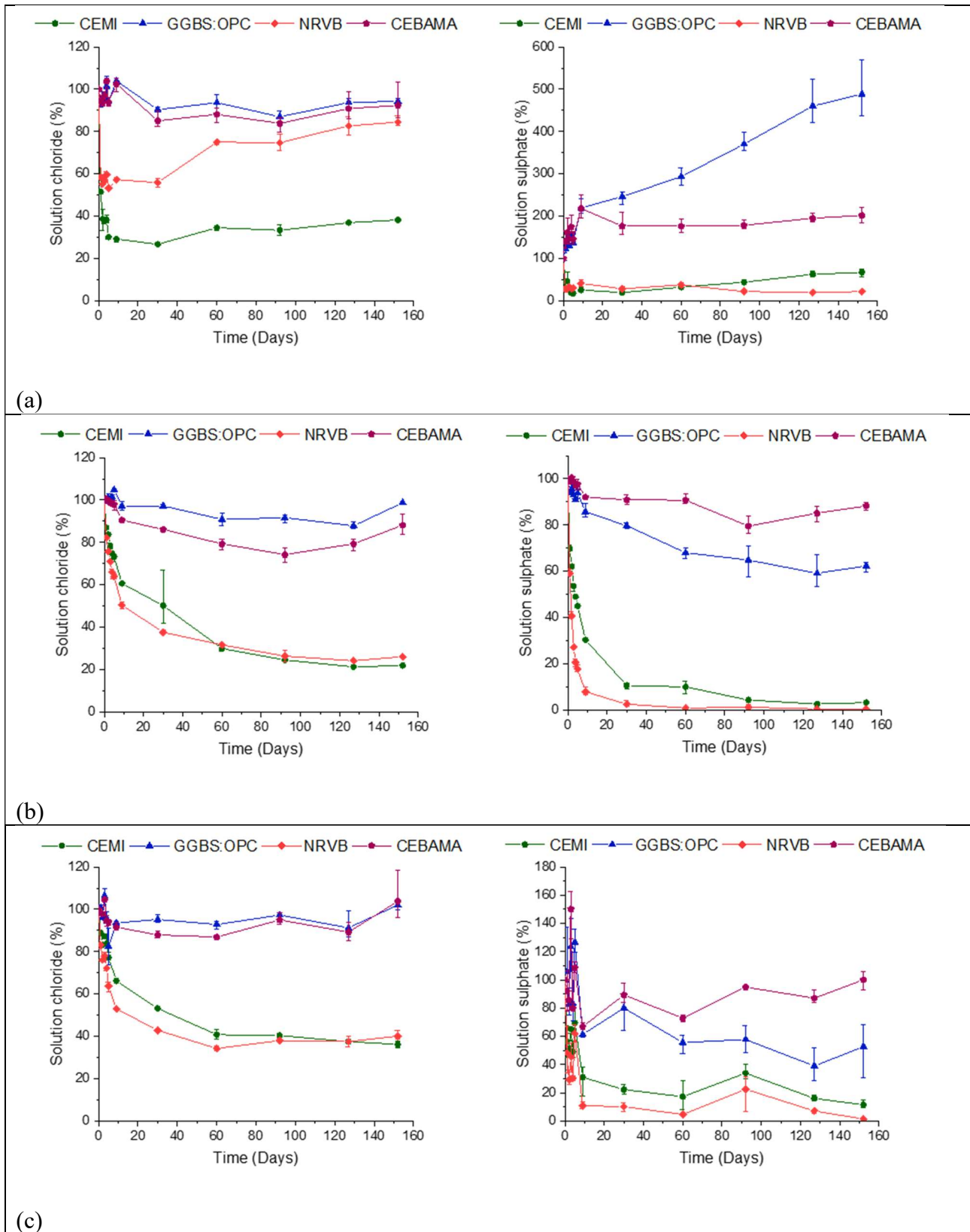


Figure 17. Changes to solution chloride and sulphate following interaction with cementitious materials. (a) granitic groundwater, (b) clay groundwater, (c) saline groundwater.

The team of CIEMAT, UAM and CSIC (Spain) analysed the chemical impact of the concrete-bentonite interaction in laboratory and in situ experiments. They concluded the impact of the cementitious materials on clay is very subtle and difficult to quantify in terms of bulk mineralogy. The altered rims affect < 2 mm in FEBEX 13 years in situ experiment, and < 0.5 mm in laboratory experiments. The alteration is mainly characterised by the precipitation of Mg-rich phases consistent with brucite intercalation in montmorillonite and saponitic compositions [Cuevas et al., 2018; González Santamaría et al., 2019; Cuevas et al., 2019a, Cuevas et al., 2019b; WP1 common paper on cement/clay interfaces;].

On the contrary, the impact of the bentonite on cementitious materials is high. Sulphate and chloride from the saturated bentonite of the in situ test diffused into the concrete inducing a significant damage that extent up to 2 and 6 cm, respectively. The kinetic of the process has been evaluated through the estimation of Cl diffusion coefficient. Mean $D_{app} = 1.6 \pm 0.6 \cdot 10^{-12} \text{ m}^2/\text{s}$ have been obtained. The mineralogical alteration is characterized by decrease of portlandite up to 2–3 cm, but not evidence of calcite increase at the interface or inside was detected respect the initial content in the FEBEX concrete plug (however, it was observed in laboratory experiment). A clear increase of ettringite up to 2–3 cm (much less in laboratory experiment) provokes alteration of the cement paste. The latter was not observed in laboratory experiments.

Regarding geochemical medium-large scale processes, they could observe a change in exchanger population of smectite in FEBEX bentonite from the in-situ test (which was largely equilibrated) and shorter laboratory tests (with a steep gradient conditioned by the thermal gradient). It was possible to deduce mass transfer when combined with highly-resolved mineralogical mapping (**Figure 18**). Na is replaced by Ca and Mg in the hot area of the HB6 test (**Figure 18**, left), while in the bentonite closest to the interface Mg is replaced by Ca, Na and K both in the in situ and lab experiments (**Figure 18**, right). The pH measured at the interface from a sample of water taken during the dismantling campaign (pH >10 promoted by the concrete) favours the precipitation of Mg-rich phases. FT-IR results indicate presence of calcite and Mg-rich phase in both experiments just at the interface.

The analysis of stable isotopes to study mass transfer (p.ej. carbonates) in the concrete-bentonite interface points to a non-homogeneous chemical environment along the concrete-bentonite interface in the in situ experiment. The calculated $\delta^{18}\text{O}$ value of the solutions in which secondary calcite was formed seem to support significant differences depending on the location of the samples in the plug. Existence of preferential flow areas would be favoured by the proximity of the granite wall and the heterogeneity of the concrete-bentonite interface itself. However, the spatial distribution of $\delta^{13}\text{C}$ values along the concrete plug and the first centimetres of the bentonite barrier demonstrate the existence of diffusion front of carbon species from bentonite towards the concrete-bentonite interface that induces the precipitation of calcite at the first millimetres of the concrete [Torres et al., 20199].

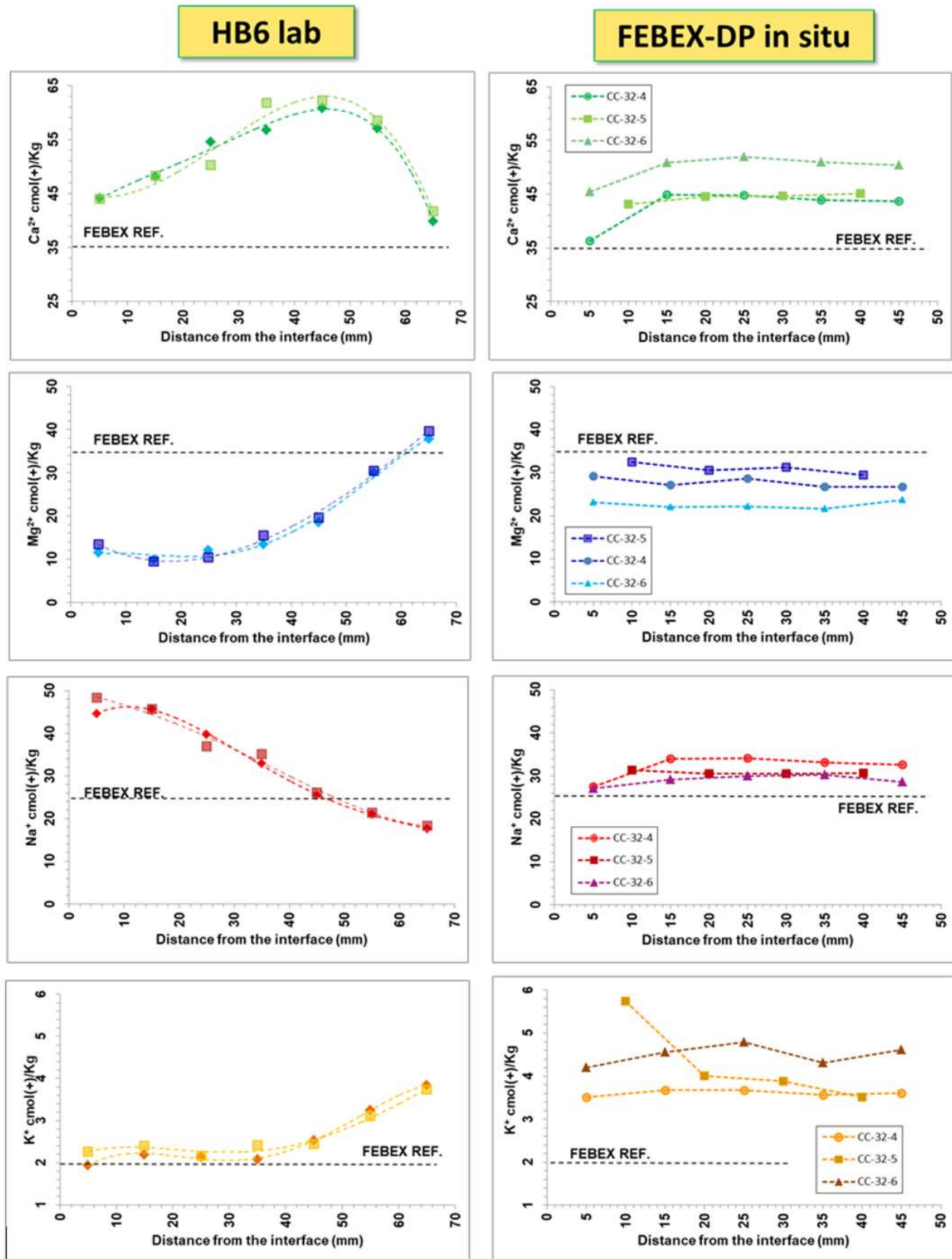


Figure 18. Exchangeable cations along the bentonite from samples of the HB6 test (left – with the tripled results) and FEBEX in situ experiment (right). Samples were taken at different distances from the interface with the concrete. Black dashed line FEBEX REF refers to the original material.

UJV_CTU team studied the behaviour and evolution of experimental solutions (composition, pH, conductivity) and pH of the leachate from studied cementitious materials. The results of the testing of geochemical behaviour confirmed the dominant influence of temperature and the type of material (OPC versus RPM). The chemistry of the GW Josef in contact with the OPC and RPM samples indicated that temperature accelerates mineral dissolution which results in increased concentrations of calcium and sulphates. In the case of the OPC samples, these ion concentrations were found to be approximately seven times higher for the heated than for the non-heated samples. Generally, the pH and total dissolved solids (deduced from conductivity) were much higher for that GW Josef exposed to OPC than that exposed to RPM (**Figure 19**).

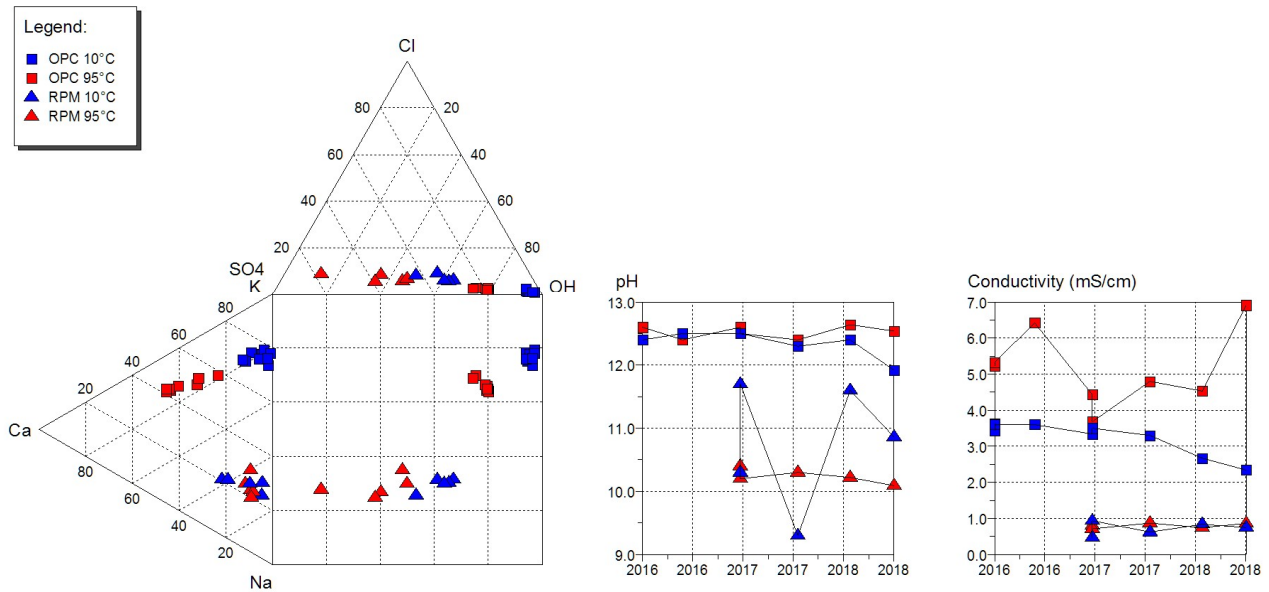


Figure 19. Chemical composition, pH and conductivity of solutions in small pressure vessels, where OPC or RPM samples were in contact with GW Josef. (CTU-UJV)

The temperature was mainly responsible for the variation in the pH of the RPM leachate samples, see **Figure 20**. The pH results of the RPM leachates are gradually approaching those observed for Cebama Reference Paste. In addition, changes in mineralogy were also influenced by temperature. In a case of RPM samples, the high-temperature completely transformed (dissolved) minerals such as ettringite and C4AF phase.

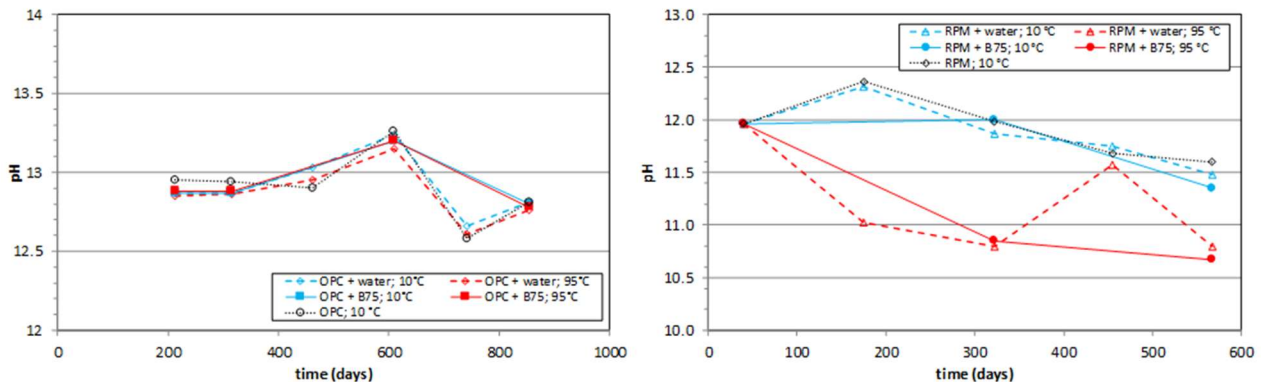


Figure 20. Time evolution of the leachate pH values of the OPC (left) and RPM (right) samples, time from casting the samples. (CTU-UJV)

3 ADVANCES IN TESTING METHODOLOGY

Testing and experimental methods have been applied in new ways during the project, which also provides advances in understanding tools for material characterization.

3.1 X-Ray Diffraction

USFD (UK) has used in-situ synchrotron X-ray diffraction to resolve kinetics of cement hydration, where X-ray diffraction patterns were taken at regular intervals over a four-year period (**Figure 21**). This method helped to understand the details of cement hydration (also as input for modelling), including porosity evolution, and also underpin subsequent leaching experiments performed on monolith samples.

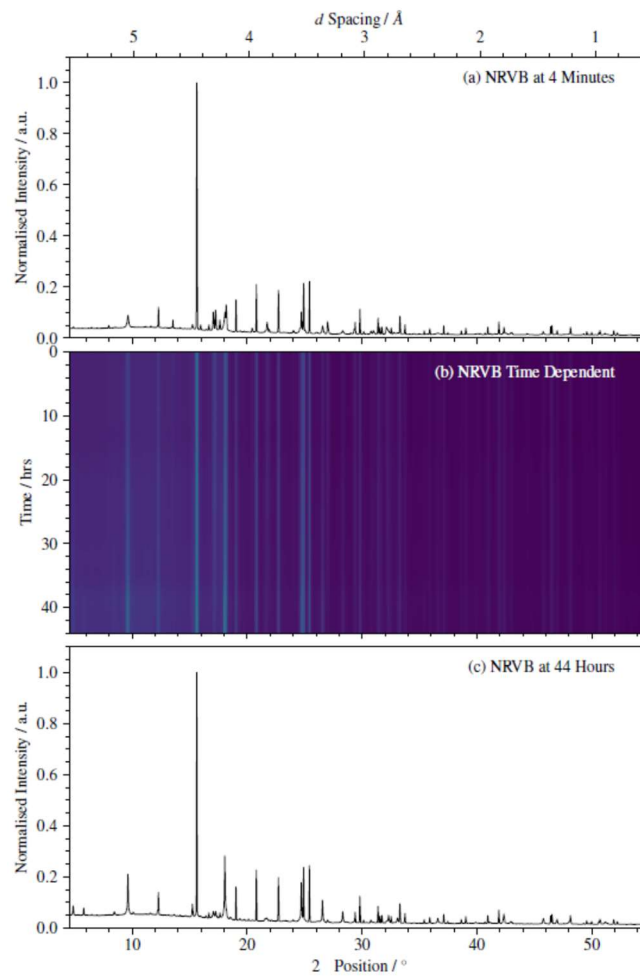


Figure 21. XRD pattern of NRVB cement materials as a function of time

At the initiation of CEBAMA project most of the studies considering water-concrete interaction consider several testing protocols to demonstrated the concrete capacity to endure leaching process and aspects related to the leachant, the solid material under study were considered critical:

- With respect to the leachant: some factors including the type of water/concrete contact regime, frequency of renewal, pressure, temperature, pH and ionic composition of the leaching solution or the liquid/solid ratio.
- With respect to the solid leaching concrete: the size and geometry of leaching material, the surface condition and porosity are important factors.
- Also the field of application and the type of scenario to reproduce real conditions affect the appropriate selection of the leaching test.

During CEBAMA large experience and knowledge has been gained with performance of full barriers instead of isolated and long-term and scale experiments respect to short-term and laboratory scale. The evaluation of long-term safety of DGR requires the analyses of the interactions at the EBS. Bentonite and concrete are main components of the EBS. The knowledge of phenomena occurring at their interface with regard the interaction of the near environment, ground waters (GW) is relevant: i) the role of ground waters and EBS pore waters in the stability of the DGR. ii) the bentonite-cementitious materials reactivity at the interface, and 3) the groundwater interaction with cementitious materials in the EBS. Besides, the experimental data used to model the long-term performance of the EBSs are generally based on simulated experiments from short-term test in laboratory. However, the scale up, differences in time and space, of the laboratory experiments respect to real-site was insufficiently supported at the starting of CEBAMA project as it is not an easy task to validate and contrast the information. So that aspects as: 1) Hydrochemical processes at concrete interface, 2) Carbonation of concrete and concrete-bentonite interface, 3) Cation exchange in montmorillonite and Mg silicates formation (Mg-Si gels: M-S-H?), 4) Dissolution of CH, development of a Ca-rich front, C-S-H evolution and C-A-S-H formation, 5) Sulfate and chloride reactions in concrete. All these mentioned processes are globally in agreement with the observations regarding realistic conditions of reaction in terms of temperature (low) and transport (mainly diffusive in concrete-clay rock interfaces): carbonation of the interface, CH dissolution, low Ca/Si C-S-H formation, and ettringite precipitation. Low pH and high pH concretes exhibited different reactivity and produce different progress in the formation of secondary phases. Some of these phases (i.e. M-S-H or C-A-S-H minerals) have not a precise chemo-structural basis for characterization, although they are detectable. The proposed experiments or in-situ aged interfaces characterisation have been focused to upgrade our understanding of the concrete-bentonite interface dynamics and to support confidence in the predictive modelling capabilities.

3.2 High-resolution PET scan

The common application of high-resolution PET-scanners is biomedical research on small animals. This requires a horizontal orientation of the scanner axis, which is often disadvantageous in geoscientific applications, particularly, when density effects have to be considered. Therefore, the method was improved by constructing a tilt mechanism and a rotary table for rotating the sample (**Figure 22**). (Jantschik et al 2019, Karimzadeh et al 2019, Kulenkampff et al 2018, Kulenkampff et al 2019).



Figure 22. Aligned vertical axes of the sample and FOV by tilting of the complete scanner. The sample is fixed on a rotary table below the gantry.

With this prerequisite the method was demonstrated on a Opalinus clay – concrete interface in a radiation-transparent pressure cell with a long-term flow experiment conducted together with University of Bern.

The capabilities of the GeoPET method were demonstrated with a measuring example from an experiment on a rock salt – salt concrete interface, which was conducted together with our partner GRS. The sample was prepared from a mature concrete core that was inserted into a matching salt rock core. The joint was flushed with concentrated salt brine until becoming impermeable by the salt precipitate. After release of the confining pressure, concentrated salt brine, labelled with ^{22}Na was given on the endplate of the sample.

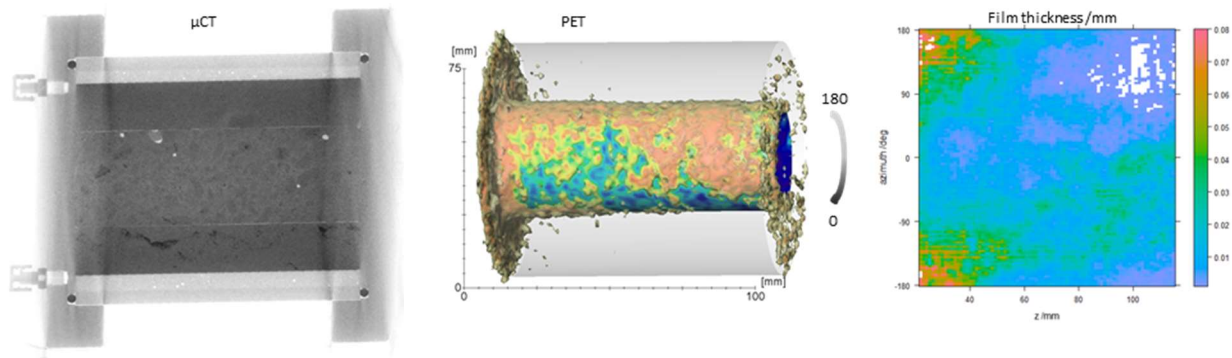


Figure 23. Experiment on a cylindrical aged salt cement insert into a halite drill core: μCT -image, initial PET-image (15 min after injection at the left endplate) and thickness map of the fluid film derived from PET activity.

In collaboration with University of Bern, GeoPET was applied to reveal the transport pathways through a Opalinus clay – concrete contact. After long-term stable injection in the innovative mobile and radiation transparent flow system of Uni Bern, the PET-nuclide ^{124}I was added to the injection fluid and the transport field was visualized with GeoPET. The first results (**Figure 24**) show that strongly heterogeneous transport has to be considered both in the clay and the cement, and – possibly similar to the former experiment on the salt-cement contact – a reservoir zone at the rock-cement contact, with a reduced transmissivity (“sealing layer”).

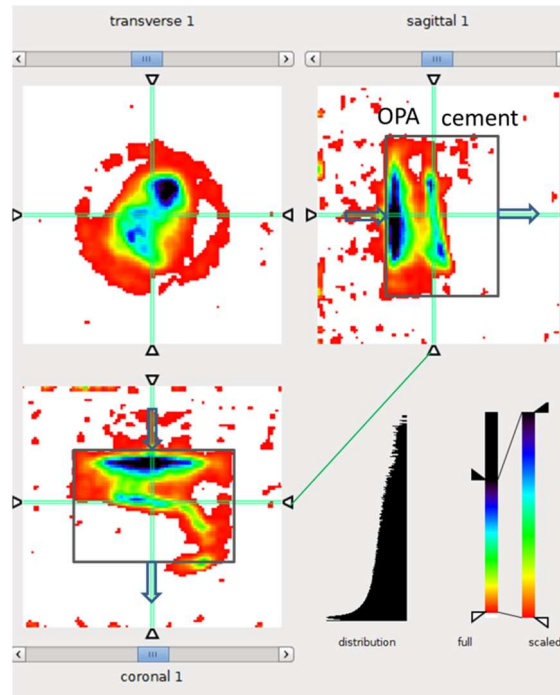


Figure 24. Tracer pattern (transversal section, horizontal and vertical longitudinal sections) 28 h after injection into a sample from the Opalinus clay – cement contact zone (qualitative image, uncorrected PET data).

3.3 X-ray CT Imaging

University of Bern (Switzerland) developed an X-ray transparent core infiltration apparatus to assess (**Figure 25**) reactive transport and mineral/porosity changes at interfaces by repeat X-ray CT imaging. This method revealed that the interface skin was less permeable than claystone and concrete. A test with low-pH mortar (ESDRED) was evaluated and yielded a distinct skin effect (**Table 2**). For a second sample (Opalinus Clay – OPC concrete), the apparatus was also transported to HZDR for additional imaging of fluid flow (see previous section) across the interface, whereby a sealing effect at the interface could be visualised.



Figure 25. X-ray transparent core infiltration apparatus. (University Bern)

Table 2. Results of hydraulic evaluation with skin effect.

	165days	39days
Δh	5 bars	10 bars
	K (m/s)	K (m/s)
ESDRED	1.5E-10	1.5E-10
OPA	2E-13	2E-13
total	7.23E-14	1.50E-14
skin	2.82E-15	5.29E-16

BRGM and SCK-CEN used methods to show the spatial distribution of porosity with a downscaling approach to create the pore network mapping for the EsB 3D stack (**Figure 26**) (Gaboreau et al. in preparation). The results of these assessments were direct inputs to the modelling tasks performed in the parallel work (workpackage 3).

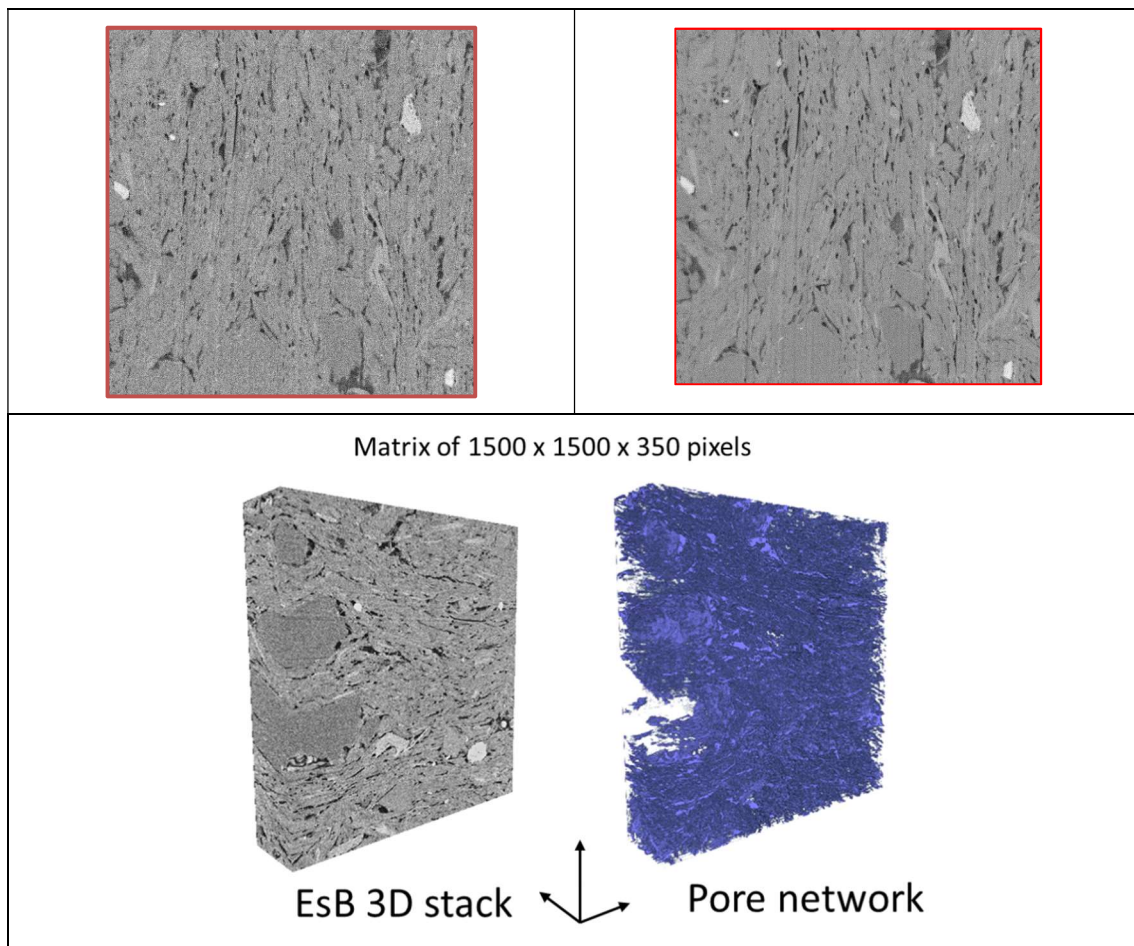


Figure 26. FIB SEM acquisition on the concrete part of the HADES in-situ interface. On the top view of images within the stack. On the bottom 3D stack and extracted pore network after applying filtering procedure. (BRGM, SCK-CEN)

4 UNDERSTANDING OF SCALE-EFFECT

A further insight was gained regarding the impact of scale and time, when reviewing the studies of CIEMAT, CSIC and UAM in Spain. **Figure 27** shows the difference in mineral perturbations and affected volume based on increasing time and scale of samples taken from the FEBEX experiment.

In what follows, in the case of concrete, secondary phase formation taken into account to define perturbation thickness was less than 10 %wt related to the original material, so it is considered always a partial alteration, as well in bentonite material. 1–3% of the shotcrete volume is perturbed in contrast to 1‰ of bentonite for the in situ case. In the case of bentonite Mg phases can predominate in a very thin rim at the concrete interface but after that rim the alteration does not affect more than 10 %wt of the original bentonite. Thus, two modes of Mg-perturbation have been established for bentonite: the zone with high concentration Mg-Phases (discrete hydroxides (hydrotalcite or brucite compositions), or chlorite-like) called high Pt (high perturbation); and a low concentration zone where mixtures of Mg-Phases and montmorillonite predominate (Low Pt, low perturbation). In the case of high Pt < 1 parts per billion of the bentonite volume is perturbed in 13 years. Other relevant data is that as the scale and time increases the perturbed volume change decrease rate: between 2 and 3 orders of magnitude for bentonite and one order of magnitude in concrete for the in situ case. In general, concrete became is more altered than bentonite [Turrero et al., 2019].

The long term and large scale experiments including Bentonite/high pH concretes have allowed to demonstrate the same mineralogical phases in concrete observed in short-term. However, the time scale indicates differences of kinetics, faster at early ages lab scale.

Certain heterogeneity was observed in the concrete plug in the in situ FEBEX experiment, despite which the geochemical processes detected at the interface are systematically repeated, and are similar to those observed in the laboratory experiment [Fernandez, R. et al., 2019].

The modification of the exchangeable cations was observed throughout the thickness of bentonite analysed (up to 5 cm). In spite of those changes no mineralogical alterations were observed. However, it would be good to consider greater thicknesses in future studies.

While bentonite properties are not extensively affected by the interaction with concrete, the concrete is affected by the interaction both with the granite (very diluted groundwater) and the bentonite (high saline porewater).

The reactivity of concrete due to bentonite salinity water transport is however largely affected by the type of concrete. A low aluminate content OPC has induced less damage in concrete for similar exposure ages (13 and 10.5 years) in contact with saturated bentonite. The formation of expansive phases inside the concrete due to bentonite water interaction depend on cement composition and initial aluminium phases in the system. The leaching of CSH in contact with bentonite evolves to rich Al gel (C-A-S-H), that can finally evolve to expansive ettringite, [Fernandez, R. et al., 2019, Torres E.,]

Long dense concretes show more durable performance than shotcrete porous concretes.

Low-pH concretes either based in silicates (OPC+SF) or aluminosilicates (OPC+SF+BFS) has shown no significant differences in short term performance [Fernandez A. et al., 2019, Alonso MC et al., 2019].

No significant changes in the physical properties of the bentonite (e.g. porosity, SSA and permeability) were found by interaction with the concrete.

The concepts and data obtained from in situ and laboratory experiments is a very robust input for modelling.

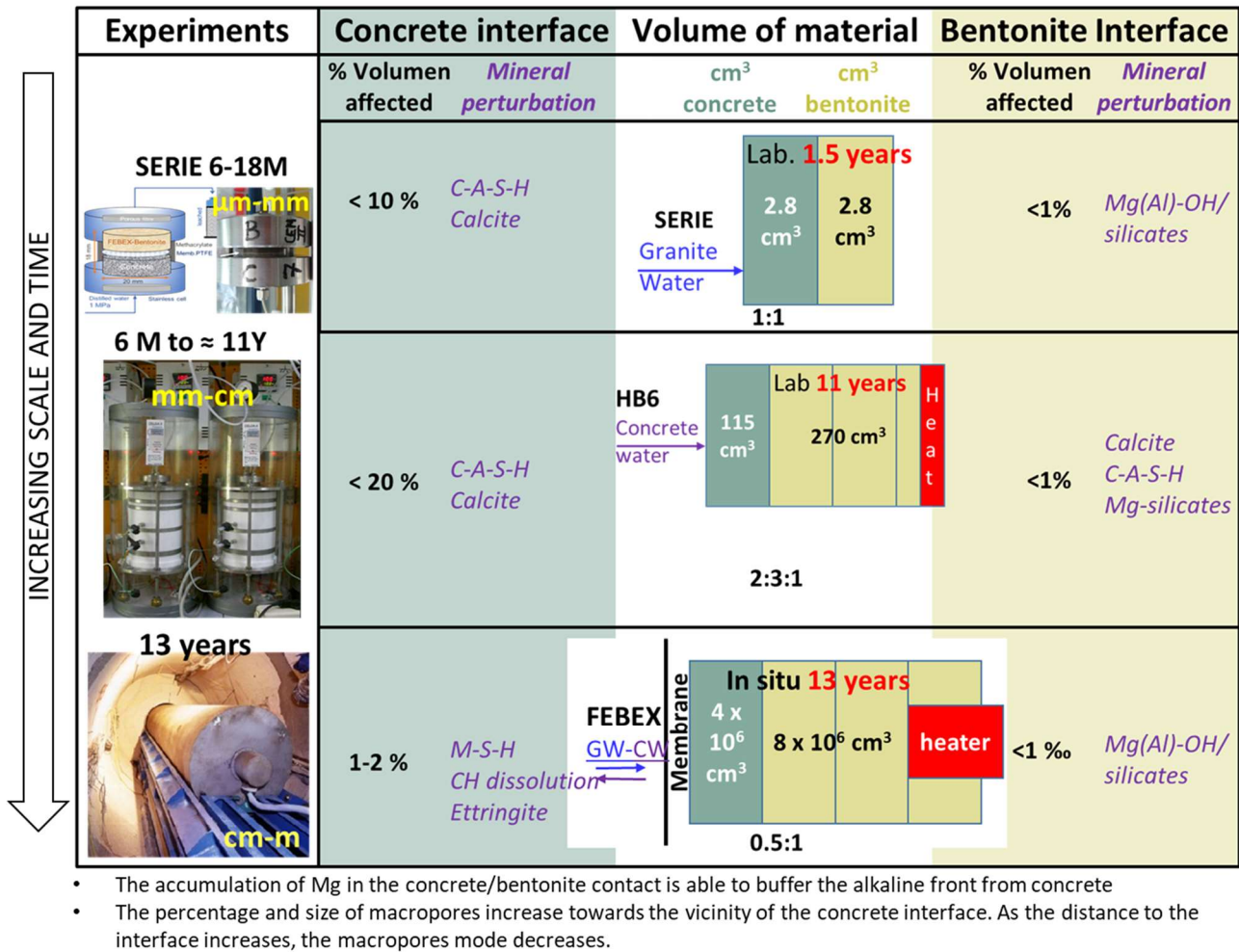


Figure 27. Concept of measurement of mineralogical-geochemical perturbation of concrete/bentonite EBS in terms of volume/volume perturbed/unaltered materials based on high pH cement concrete interactions. Volumes taken on EBS are those constrained in the laboratory experiments and those relative fixed between FEBEX projected shotcrete and the active heater.

5 CONCLUSIONS

The work of 19 partners from 12 countries have made strong advances in understanding of the THMC processes at the cement-clay interfaces and how it impacts the engineered barrier system (EBS) evolution.

Key summary points regarding the claystone and bentonite interfaces with OPC and low-pH cementitious materials are that:

- there is very little clay alteration in the early ages (0–14 years); the mineralogical changes are at mm scale; there is only selective mass transfer up to 1–2 cm (Mg, S)
- porosity (and mass) re-distribution occurs at a small scale; there is only a partially coherent pattern; there is indication for a tendency of permeability reduction (H, D)
- there is no distinct difference between the extent of (clay) alteration and type of cementitious material (OPC, low-pH) at low temperature
- cement-internal extent of alteration in low-pH material is at least as extensive as in OPC (though it is difficult to compare due to many parameters)
- there no compelling reason for not using OPC from chemical/mineralogical perspective
- if skins are effective: delays in bentonite hydration, and possible reduced gas-escape
- there is a relatively robust understanding of key processes in all systems
- there are a wide range of mature and tested analytical and experimental techniques available.

The results from this project are useful to the end users of waste management organizations in many ways. The results are used for design issues, with respect to:

- feeding into specifications about how the repository is designed,
- aiding specification/selection of material parameters, material compatibility, evolution
- aiding specifications for experimental methods, i.e. for material quality control.

The results are also used for safety evaluation by end users, accounting for the evolution of the system. The following conclusions are drawn from this project and the experimental studies that aid the safety assessment:

- interfaces (concrete-bentonite-host rock) can co-exist safely
 - there is a better understanding of impacts from material interface processes for realistic description of the system performance
 - there is an understanding how the interface can affect strength, flow properties, etc.
 - transport processes have a variation with time
 - there is evidence of porosity changes, though information on if and when clogging occurs should be further studied
 - there is improved accuracy in robustness and weighting of safety functions,
 - there is increased modelling accuracy with new data and process understanding (use for the modelling work package from this project).
-

6 REFERENCES

- Alonso MC, Fernandez, A. and Garcia-Calvo, J.L. 2018. Ground-water composition in the interaction with low-pH OPC-SF based concrete, Cement based materials for nuclear waste, NUWCEM, Avignon France
- Bentz, D.P., Jensen, O.M., Coats, A.M., Glasser, F.P., 2000. Influence of silica fume on diffusivity in cement-based materials: I. Experimental and computer modeling studies on cement pastes. *Cement and Concrete Research* 30, 953–962.
- Codina, M., Cau-dit-Coumes, C., Le Bescop, P., Verdier, J., Ollivier, JP. 2008. Design and characterization of low-heat and low-alkalinity cements. *Cement and Concrete Research* 38:437–448.
- Cuevas, J., Ruiz, A.I., Fernández, R., González-Santamaría, D., Angulo, M., Ortega, A., Torres, E., Turrero, M.J. 2018. Authigenic Clay Minerals from Interface Reactions of Concrete-Clay Engineered Barriers: A New Perspective On Mg-Clays Formation in Alkaline Environments. *Minerals*, 8, 362, 1–18. doi:10.3390/min8090362.
- Cuevas, J., Angulo, M., González-Santamaría, D.E., González-Yelamos, J., Fernández, R., Ortega, A., Ruiz, A.I. 2019a. High pH concrete FEBEX-bentonite interface reactions: from months to decades and from cm³ experiments to m³ in-situ scenario. Proceedings of the Second Workshop of the HORIZON 2020 CEBAMA Project. ISSN 1869-9669, ISBN 978-3-7315-0825-0. KIT Scientific Reports 7752. KIT Scientific publishing. Karlsruhe 125–132.
- Cuevas, J., Angulo, M., González-Santamaría, D.E., González-Yelamos, J., Fernández, R., Ortega, A., Ruiz, A.I. 2019b. Time and spatial scales observation of chemical profiles arising from surface interaction of bentonite in different cement environments. Proceedings of the third Workshop of the HORIZON 2020 CEBAMA. In press, to be published with the final report. 8 pp.
- Dauzeres, A., De Windt, L., Detilleux, V. 2017. Geochemical evolution of cementitious materials in contact with a clayey rock at 70 C in the Tournemire underground research laboratory. KIT Scientific Reports. Proceedings of the Second Workshop of the HORIZON 2020 CEBAMA Project.
- Fernández, R., Ruiz, A.I., Ortega, A., Torres, E., Angulo, M., González-Santamaría, D.E., Fernández, A., Alonso, M.C., Turrero, M.J., Cuevas, J. 2019. Geochemical perturbations in the contact between concrete and bentonite after 13 years of interaction at microcentric to centrimetric scales, 5th Int WS on Mechanisms of waste/Cement Interactions, CEM2019, Karlsruhe.
- Fernandez A., Alonso MC, Garcia-Calvo, J.L. 2019. Effects of different groundwaters interaction in high and low pH concretes. To be published in *Cement and Concrete Research*.
- Gaboreau, S., Phung, Q.T., Francis, C., Maes, N. In preparation. Multiscale characterization of the spatial heterogeneities of microstructure and mineralogical evolution of 14-year in-situ concrete-clay interfaces. *Applied Geochemistry*.
- González Santamaría, D.E., Fernández, R., Ruiz, A.I., Cuevas, J. 2019. Bentonite/CEM-II concrete INTERFACE EXPERIMENTS: a proxy to an in situ DGR engineered barrier system surface reactivity. (*Applied Geochemistry*, to be submitted before August 2019).
- Jantschik, K., Kulenkampff, J., Lippmann-Pipke, J., Moog, H.C. 2019 (in preparation). Investigation the sealing capacity of the contact seam of a cement-based sealing element in rock salt. Target journal *Cement and Concrete Research*.
-

Karimzadeh, L., Kulenkampff, J., Schymura, S., Lippmann-Pipke, J., Fischer, C. 2019 (in preparation). GeoPET/ μ CT tomography technique in reactive transport modelling. Target journal *Nature Geoscience*.

Koskinen, K., 2014. Effects of Cementitious Leachates on the EBS, Posiva Oy, Working Report 2013-4, 63 pp.

Kulenkampff, J., Franke, K., Gründig, M., Hildebrand, H., Karimzadeh, L., Schymura, S., Fischer, C. 2018. An experimental approach to reactive transport in geomaterials: GeoPET. Oral, RadChem, Mariánské Lázně, Czech Republic, 13.-18.05.2018.

Kulenkampff, J., Jantschik, K., Gründig, M., Moog, H., Lippmann-Pipke, J. 2019. (in preparation). Process tomography for testing the sealing efficiency at the rock cement contact. Target journal *Geotechnique*.

Lalan, P., Dauzères, A., De Windt, L., Bartier, D., Sammaljärvi, J., Barnichon, J-D., Techer, I., Detilleux, V. 2016. Impact of a 70 °C temperature on an ordinary Portland cement paste/claystone interface: An in situ experiment. *Cement and Concrete Research* 83:164–178.

Phung, Q.T., Maes, N. 2019. In preparation. Evolution of transport properties of saturated cementitious materials subjected to combination of carbonation and leaching. Target journal *Materials*.

Phung, Q.T., Diederik, J., Maes N. 2019. In preparation A continuum model coupled diffusion, microstructure and geochemical to describe combined carbonation-leaching of cement pastes in a clay environment. Target journal *Applied Geochemistry*.

Torres, E., Turrero, M.J., Garralón, A., Cuevas, J., Fernández, R., Ortega, A., Ruíz, A.I. 2019. Stable isotopes applied to the study of the concrete-bentonite interaction in the FEBEX in situ test. *Applied Geochemistry*, 100, 432-443. <https://doi.org/10.1016/j.apgeochem.2018.12.017>

Torres, E., Turrero, M.J., Garralón, A., Fernández, R., Ruíz, A.I., Ortega, A., M.C. Alonso, A. Fernández, J. Cuevas, (2019). Progresion of the geochemical interaction at the concrete-bentonite interface under simulated engineered barrier conditions, 5th Int WS on Mechanisms of waste/Cement Interactions, CEM2019, Karlsruhe.

Turrero, M.J., Cuevas, J., Alonso, M.C., Fernández, A., González-Santamaría, DE., Fernández, R., García-Calvo, JL., Ruiz, AI., Torres, E. 2019. Ground waters interaction with EBS for HRW: from laboratory to in-situ spatial and time scale up. 5th Int WS on Mechanisms of waste/Cement Interactions, CEM2019, Karlsruhe.

Vašíček R., Červinka R., Večerník P., Rosendorf T., Svoboda J. 2018. Geochemical and Thermal Impacts on the Characteristics of Cementitious Materials: Strength, Leachate pH, mineralogy and Diffusion. S&T paper, 3rd Annual Workshop of the Cebama project, 17th - 18th April, 2018 Nantes, France.

Večerník P., Hausmannová L., Červinka R., Vašíček R., Roll M., Hloušek J., Havlová V. 2016. Interaction between cement and Czech bentonite under temperature load and in in-situ conditions: an overview of experimental program. CEBAMA 1st Annual Workshop.

Vehmas T., Holt E. (editors).2016. WP1 Experimental studies – State of the art literature review (Chapter 5.1 Havlova, V., Vecernik, P.: Diffusion of species through cement materials), CEBAMA Deliverable D1.03, KIT Germany.

Vehmas T., Itälä, A., Heikola, T., Leivo, M., Holt E., Vuorio, M.. 2017. Cementitious leachates interaction with MX-80 bentonite in geological nuclear waste repository environment. 7th International conference on clays in natural and engineered barriers for radioactive waste confinement, 24th-27th of September, Davos, Switzerland

Vehmas T., Leivo M., Holt E.. 2016. Comparison of experimental and modelled results of low-pH Ordinary Portland Cement systems, Nordic Concrete Research seminar -Concrete for Nuclear Structures NUCCON 2016, Espoo, Finland, 31 October – 1 November 2016.

Vehmas T., Leivo M., Holt, E.. 2017. Comparison of experimental and modelled pore solutions of low-pH ordinary Portland cement based mix designs. XXIII Nordic concrete research symposium proceedings, 21st-23rd of August, Aalborg, Denmark.

Vehmas T., Leivo, M., Holt, E. 2019. Comparison of Experimental and Modelled Leaching of Cementitious Materials in Nuclear Waste Repository Environment (in preparation) *Applied Geochemistry*.
